ASSESSING MUSCLE MICROSTRUCTURE THROUGH QUANTITATIVE MAGNETIC RESONANCE IMAGING FOLLOWING HAMSTRING STRAIN INJURY

By

Christa Wille

A dissertation submitted in partial fulfillment

of the requirements for the degree of

Doctor of Philosophy

(Biomedical Engineering)

at the

UNIVERSITY OF WISCONSIN-MADISON

2023

Date of final oral examination: May 18th, 2023

The dissertation is approved by the following members for the Final Oral Committee:

Bryan Heiderscheit, Professor, Orthopedics and Rehabilitation and Biomedical Engineering

Darryl Thelen, Professor, Mechanical Engineering and Biomedical Engineering

Mary Elizabeth Meyerand, Professor, Biomedical Engineering and Medical Physics

Kenneth Lee, Professor, Radiology

Geoffery Baer, Professor, Orthopedics and Rehabilitation

I dedicate this thesis to my girls who have not only given me my most important title, but have also given me unending love, joy, and fulfillment as I have sought after the title this document brings. To my husband, Eamon, for his patience, love, and understanding throughout my academic journey, and to my parents for their lifetime of unrelenting support and love through all of my endeavors.

Acknowledgments

The work in this thesis would not have been possible without the guidance and contributions from many others. First, I would like to thank my primary advisor, Dr. Bryan Heiderscheit, who introduced me to the field of biomechanics and developed in me a strong sense of exploration to probe the unknown, challenge ambiguous concepts, and discover relevant solutions. Your patience, guidance, and encouragement has driven me to be a better scientist, clinician, and educator.

Thank you to my committee members—Drs. Darryl Thelen, M. Elizabeth Meyerand, Kenneth Lee, and Geoffery Baer—for their time, dedication, and feedback that has guided me not only through the completion of this thesis, but also through all that life has presented me with over the last several years.

I offer a sincere note of thanks to Dr. Samuel Hurley who unknowingly took on a physical therapist interested in muscle injuries, and willingly taught her a wealth of knowledge related to Medical Physics. Thank you for your patience and your ability to explain challenging concepts (often more than once) in easily comprehendible ways. Your passion and knowledge related to Medical Physics is remarkable, your generosity and willingness to share that knowledge with others is inspiring, and the companionship you have provided me through these challenging times will stay with me long beyond the hours, days, and years it has taken me to complete this document.

To the lab members within Badger Athletic Performance, thank you for sharing with me the day-in-and-day-out challenges and joys of research in sports medicine. Thank you especially to Dr. Mikel Stiffler-Joachim who helped facilitate the data collections for each of the student athletes included in these analyses. To Dr. Stephanie Kliethermes—a heartfelt thank you for your time and willingness to share with me a portion of your refined knowledge related to statistical analyses and study design. Thank you, also, to the undergraduate and graduate

students, especially Elizabeth Schmida, for the contributions they have made assisting with the preparation of the imaging data used in these analyses. Finally, I would like to acknowledge the UW Athletics Sports Medicine staff and the student athletes themselves.

This work would not have been possible without the funding sources that foresaw the value in these investigations and supported me in my education and training. The NBA & GE HealthCare Orthopedics and Sports Medicine Collaboration (MYT-015, D223), and those that at the University of Wisconsin Institute for Clinical and Translational Research and the National Institute of Health through award number TL1TR002375. The content is solely the responsibility of the authors and does not necessarily represent the official views of the NIH.

Most importantly, I would like to thank my village—the strong network of friends and family that have support me and my growing family through these years. Your understanding, encouragement, and assistance continues to be greatly appreciated.

Table of Contents

Abstract

Diffusion tensor imaging (DTI) holds promise in the evaluation of muscle microstructure. While DTI may be beneficial in the management of muscle strain injuries, specifically of the hamstrings, the interpretation of DTI-derived measures of muscle microstructure applied to injured muscle is complex and associations with clinical outcomes remain unknown. [1, 2]The purpose of this thesis was to implement DTI to monitor muscle microstructure changes and to explore the association of DTI-derived measures of microstructure with clinical outcomes following acute hamstring strain injury (HSI).

Imaging and clinical outcomes were collected from athletes who sustained an HSI at time of injury (TOI), upon clearance for return to sport (RTS), and 12-weeks after RTS. In Chapter 2, we explored methods to define the injured region and observed between-limb differences in microstructure over time. Further, exploration of clinical associations of DTI-derived muscle microstructure was done alongside conventional measures of injury and muscle morphology. While Chapter 3 explored the association of TOI imaging measures with clinical outcomes such as time to RTS and reinjury incidence, Chapter 4 used RTS imaging measures to explore clinical associations with eccentric hamstring strength and reinjury incidence.

When the region of injured muscle tissue is defined by a volume of increased signal in a T2-weighted image at TOI and registered imaging data at subsequent time points, between-limb differences in muscle microstructure are apparent at TOI but not at follow-up time points. Exploration of clinical associations with TOI imaging measures did not detect an association with days to RTS. Similarly, measures of injury and muscle morphology did not demonstrate an association with reinjury incidence. Unexpectedly, those who went on to reinjure demonstrated decreased quantitative diffusion parameters consistent with a less severe injury at TOI compared to those who do not reinjure. Analysis of microstructure at RTS demonstrated the between-limb comparison of DTI-derived parameters (radial diffusivity, and λ_1) held a significant

association with between-limb eccentric hamstring strength. Conversely, between-limb measures of injury and muscle morphology were not associated with strength.

The overall findings from this thesis indicate DTI-derived measures of muscle microstructure can be used to describe between-limb differences following HSI. Additionally, muscle microstructure identified with DTI may be more closely linked with clinical outcomes, such as eccentric strength, than measures of muscle morphology in injured hamstring muscle.

Chapter 1.

Introduction

Magnetic Resonance Imaging in the Management of Muscle Injuries

Magnetic resonance imaging (MRI) is routinely used to aid in soft tissue injury management and prognosis in a sports medicine setting. Due to its ability to visualize soft tissues with excellent contrast, provide high spatial resolution, and multiplanar assessment, MRI is considered the reference imaging method to assess morphology in athletes.[3] Conventional MRI sequences have been tailored for the qualitative evaluation of pathologic abnormalities.[4] However, as the rate of MRI studies and musculoskeletal applications continues to expand, quantitative MRI applications are gaining interest and are frequently being used to complement qualitative imaging with more detailed information, providing measures that could aid in earlier diagnosis, increased accuracy for prognosis, or as a tool to monitor tissue following injury or intervention.[4]

Various MRI-based classification systems have been proposed as a means to incorporate both qualitative and quantitative assessment of muscle injury by identifying and evaluating the extent and severity of injury.[5-9] Categories used to classify injuries include: mechanism and location of injury, number of muscles involved, length of edema, estimated cross sectional area, and peak hyperintensity signal. One classification system becoming more widely implemented is the British Athletics Muscle Injury Classification (BAMIC) system,[6] which uniquely combines both an assessment of injury severity with a 0-4 grading system, and identification of the injury location based on the anatomical site within the muscle and the tissue structures involved (myofascial [a], myotendinous [b], intratendinous [c]). The utility of BAMIC as a tool for accurately determining prognosis following muscle injury is debated. While many prior studies have demonstrated a significant relationship exists between BAMIC injury classification

and clinical outcomes such as time to return to sport (RTS)[10-13] or reinjury incidence,[12, 14] several did not detect a relationship between BAMIC and days to RTS[14-16] or BAMIC and reinjury.[13] Thus, the validity of injury classification systems to aid in prognosis and long-term clinical outcomes remains limited.[16]

While measures of injury classification systems such as BAMIC quantify changes in muscle tissue structure at the gross-anatomical level of muscle, early (patho-)physiological changes may start at the cellular or fascicular level. Recent improvements in advanced measures of quantitative MRI, such as diffusion weighted imaging (DWI), have emerged as promising methods to monitor muscle microstructure at the cellular level.[17] Furthermore, early applications of DWI in the context of muscle injury or damage demonstrate that DWI may be able to detect micro trauma that remained undetected with conventional T1- or T2-weighted imaging.[1, 2]

Diffusion Weighted Imaging

Background

Diffusion, in biological tissue, describes the Brownian motion of water molecules. The characterization of diffusion has the capability to portray tissue microstructure, and when applied in a pathological setting, it may be able to distinguish changes in tissue microstructure.[10, 18-20] While DTI is an established technique in neuroradiology, the application of DTI in skeletal muscle is relatively new. However, the well-known fascicular organization of skeletal muscle, from the microscopic to macroscopic level, makes DTI suitable for the evaluation of muscle.

Theory and Acquisition

In DWI, the amount of diffusion is quantified by the diffusion coefficient. In biological tissue, diffusion can be hindered by a range of factors including physical barriers like cell membranes. Thus, in a biological setting diffusion is described by the apparent diffusion coefficient (ADC) to discriminate it from unhindered diffusion.[17] DWI is typically performed using a single-shot diffusion-weighted spin echo echo planar imaging pulse sequence.[21] It uses a pair of magnetic field gradients, placed on either side of the refocusing pulse, to encode diffusion (**Figure 1.1**). The first gradient application disperses the phases of the protons' magnetic moments, while the second gradient tends to restore phase coherence. If transverse relaxation processes are ignored, the protons' phase coherence is completely restored for stationary water molecules and incompletely restored for diffusing water molecules. The incomplete phase restoration for diffusing water molecules causes the MRI signal to decay exponentially with increasing displacement (Equation 1), and is described by a scalar diffusion coefficient that is sensitive only to diffusion along the direction of the gradient.[22] Alternative DWI acquisition sequences include stimulated echo pulse sequences, Turbo Spin Echo, or multi-shell diffusion imaging [23-25] but require additional acquisition and post-processing resources limiting the clinical utility of these methods. Thus, the most available, fast, and robust sequence for acquiring DTI skeletal muscle is single-shot diffusion-weighted spin echo echo planar imaging.[26]

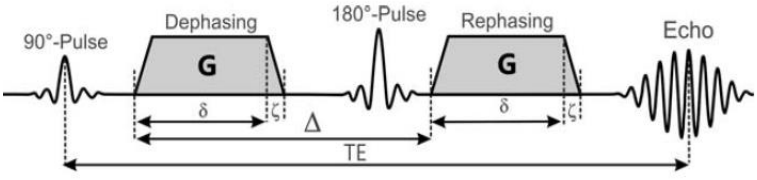

Figure 1.1. Schematic representation of a diffusion-weighted Stejskal-Tanner pulsed gradient spin echo sequence, with: **G** the gradient strength, δ the gradient duration, ζ the rise time of the gradients, and Δ the delay between the leading edges of the two pulsed field gradients. Adapted from Oudeman et al.[17]

Regardless of the acquisition method, diffusion sensitizing is accomplished by using diffusion gradients that cause signal attenuation. The resulting signal intensity is related to the ADC [mm^2/s] by:

$$S_b = S_0 e^{-bADC} \qquad (1)$$

Where S_b is the diffusion-weighted signal and S_0 the non-weighted signal, the b is the b-value, which is the amount of diffusion weighting and depends on the gradient strength G and gradient timing.[27] In order to ensure a sufficient signal-to-noise ratio (SNR) when collecting DWI of skeletal muscle, it is recommended to use a short echo time, a b-value between 400-500 s/mm^2, and to use at least gradient directions.[28] The typical acquisition time ranges between 5-10 minutes but will depend on the number of slices, the specific application, the size of the muscle, and the available hardware (e.g., strong gradients, specialized coils).

Diffusion Tensor Imaging

With additional gradients applied along multiple directions, it becomes apparent that in some tissues and organs water diffusion exhibits directional dependence. This observed diffusion anisotropy occurs because for cells with elongated geometries, water preferentially diffuses along the long axis of the cell. Given the preferential directional diffusion in organs such as muscle, a scalar diffusion coefficient is not sufficient to describe the diffusion, and thus tissue microstructure of muscle. By measuring the ADC in at least six independent directions, DWI can be used to quantify the directional anisotropy of diffusion. Instead of a scalar ADC parameter, the diffusivity is then described by a three-by-three tensor ***D*** (equation 2)—hence the name diffusion tensor imaging (DTI).

$$D = \begin{bmatrix} D_{xx} & D_{xy} & D_{xz} \\ D_{xy} & D_{yy} & D_{yz} \\ D_{xz} & D_{yz} & D_{zz} \end{bmatrix} \quad (2)$$

Diagonalization of the tensor provides the eigenvalues and eigenvectors used to describe the tensor, with three orthogonal eigenvectors ($\vec{\varepsilon}_1, \vec{\varepsilon}_2, \text{and } \vec{\varepsilon}_3$) describing the principal diffusion directions and their corresponding eigenvalues ($\lambda_1, \lambda_2, \text{and } \lambda_3$) describing principal effective diffusivity. Eigenvalues are positive and ordered $\lambda_1 \geq \lambda_2 \geq \lambda_3$, with the principal eigenvector (λ_1) representing the direction with the highest diffusion, shown to correspond to local muscle fiber orientation.[29] Combining principal diffusion direction of neighboring voxels can be used for three-dimensional muscle fiber tractography.[22, 30]

To allow for further interpretation of the diffusion tensor, several rotation and scaling invariant scalar indices have been introduced to enable a quantitative comparison that can be made between measurements and across subjects. Mean diffusivity (MD) is an index that describes the directional average (equation 4) of the diffusion in the tissue.

$$MD = \frac{(\lambda_1 + \lambda_2 + \lambda_3)}{3} = \bar{\lambda} \quad (4)$$

Radial diffusivity (RD) is an index that describes the transverse average (equation 5) of the diffusion in the tissue.

$$RD = \frac{(\lambda_2 + \lambda_3)}{3} \quad (5)$$

Fractional anisotropy (FA) is a measure used to quantify diffusion anisotropy (equation 6).[31] FA is dimensionless and equals 0 for isotropic medium and approaches 1 for a cylindrically symmetric anisotropic medium.

$$FA = \sqrt{\frac{3}{2}} \frac{\sqrt{(\lambda_1 - \bar{\lambda})^2 + (\lambda_2 - \bar{\lambda})^2 + (\lambda_3 - \bar{\lambda})^2}}{\sqrt{\lambda_1^{\,2} + \lambda_2^{\,2} + \lambda_3^{\,2}}} \quad (6)$$

The values of the diffusion tensor components and scalar parameters can be biased by low SNR,[28, 32] thus care should be taken to optimize acquisition parameters. Similarly, it is important to minimize the effects of artifacts commonly associated with DTI (e.g., susceptibility-related artifacts, eddy current distortions, motion artifacts, and chemical shift).[17, 26] Proper shimming and increasing the echo planar imaging bandwith in the phase-encoding direction can reduce susceptibility-induced deformations[33] while remaining deformations can be further decreased by correcting distortion, eddy current, and motion artifacts[34] and denoised using a local principal component analysis filter.[35]

Tractography

In addition to the quantification of muscle microstructural properties, DTI can be used to visualize the architecture of muscle tissue by combining principal diffusion direction of neighboring voxels for three-dimensional muscle fiber tractography.[22, 30] Fiber tractography is often started from a selected region of interest and continues until a cutoff value is reached. Common cutoff values are a minimal and maximal FA and the angular change of the fiber tract per integration step.[36] Fiber tractography allows for the quantification of architectural parameters such as pennation angle, curvature, fiber length, and physiological cross-sectional area.

Applications in Muscle Injury

While T1- and T2-weighted images can monitor and quantify changes in muscle tissue structure due to (patho-)physiological conditions such as inflammation, trauma, or atrophy at the gross-anatomical scale, early or more subtle changes often occur at the cellular or fascicular level which is beyond the capability of standard imaging.[17] This also means that it may be

challenging to monitor lingering signs of injury or early signs of tissue adaptations following intervention not clinically evident or visible on standard imaging techniques.[17] Microstructural (cell-level) changes that have been observed with injury include fiber atrophy/hypertrophy,[37] fibrosis,[38] membrane damage (permeable fibers),[39] and edema.[23] Common methods to study injury-associated changes following injury include histology[40] and ultrasound imaging.[41] While histology is limited significantly by its highly invasive nature, both histology and ultrasound methods are limited significantly by their field of view and are often difficult to extrapolate to the entire muscle. Therefore, DTI as a quantitative, noninvasive technique to study muscle microstructural changes resulting from injury may hold potential in the clinical assessment of muscle pathologies.

Previous work has demonstrated that DTI is sensitive to changes in muscle microstructure that may not be detected in other T2-weighted imaging sequences.[1, 2, 18] In the presence of muscle injury, less restricted diffusion is expected due to compromise of structural integrity of the sarcolemma, which affects the permeability of water exchange between intra- and extracellular compartments. This would be consistent with changes in diffusivity parameters including increased diffusivity in principal eigenvalues (λ_1, λ_2, λ_3), increased MD, RD, and decreased microstructural organization (FA).

Although physiological processes reflected as changes in muscle tissue diffusivity have been previously observed using DTI in humans following exercise[1, 2, 42] and acute muscle strain injury,[10, 19, 20] the relationship among tissue microstructure, actual diffusion changes, and the resultant diffusion tensor is complex.[25] While increased diffusivity in the presence of muscle injury may be easily explained by muscle membrane damage, other known effects of injury including, increased extracellular fluid associated with edema, or the increased permeability to water exchange between the intra- and extracellular compartment may also contribute to increased diffusion.[37, 43] Advanced techniques to improve the specificity of DTI

to measure microstructural changes in the presence of injury include more averaging or increased diffusion-gradient directions[28, 32] to increase SNR or multi-shell diffusion imaging,[23-25] multi-exponential T2 quantitative mapping,[25] and muscle specific model fitting.[44] However, the clinical implementation of these techniques is limited by sequence optimization and protocol times when imaging a relatively large muscle. Nonetheless, using a clinically feasible single shot echo echo planar imaging diffusion sequence, certain structural quantities averaged over an ROI have been shown to serve as a proxy for structural features and their changes in the presence of muscle injury in humans.[18, 19]

Current practices rely on the presence of edema to define the injured region, further complicating the interrelationship between diffusion parameter outcomes being driven by changes in structural integrity and/or the presence of extracellular fluid. Although the majority of prior studies have chosen a focal, representative ROI within the edema region to represent injury,[10, 18-20] a consensus has not been reached to consistently or repeatably define this region. One unique approach to define an injured region that can be replicated across consecutive follow-up timepoints is to anchor the ROI to the axial slice with the greatest cross-sectional area of edema and analyze a consistent number of slices above and below.[18] Each of these methods requires a subjective input that may limit the consistency in comparison across subjects and across studies. A more thorough understanding of how ROI definition influences observed changes in diffusion parameters, both at TOI and at follow-up time points, would aid in the utility of DTI for evaluating acute HSIs.

Although initial evidence demonstrates that DTI is sensitive to detect differences in the injured limb following acute muscle injury,[18] the association of DTI parameters following acute injury and longitudinal clinical outcomes such as time to RTS, muscle function as a measure of recovery, and reinjury incidence has not yet been explored.

Magnetic Resonance Imaging in the Management of Hamstring Strain Injuries

Muscle injuries represent a major challenge for recreational and elite athletes alike, accounting for approximately of one-third of all sports-related injuries.[45-47] Of those, injuries to the hamstring muscle complex are among the most prevalent, comprising upwards of 37% of all muscle injuries.[45] Hamstring strain injuries (HSI) result in significant loss of time from activity, decreased quality of life,[48] and increased financial burden in elite sports [49]. Management of HSIs is further complicated by limited prognostic indicators[50] and high rates of reinjury spanning from 32-64%.[51, 52]

While HSI are often clinically diagnosed and managed, MRI has become increasingly available and utilized, especially in collegiate and professional athletes with HSI.[53, 54] However, the prognostic value of MRI-based assessments within days following an acute HSI is widely debated.[15, 55-58] The majority of MRI-based measures used to determine injury prognosis thus far are at the gross anatomical level (i.e., volume, location, number of muscles involved),[58] and do not appear to improve predicting time to RTS beyond physical examination metrics and athlete HSI history.[15, 59] Conversely, there is a growing body of evidence supporting the association between MRI-based injury grading scales, such as the BAMIC, and time to RTS.[10-12, 14, 60] While several indicate BAMIC holds a significant predicative ability for RTS assessment,[10, 12, 13] others question the clinical utility of the identified relationship[11, 14, 15] likely due to the large variability[15] and influence of external factors associated with time to RTS following HSI.

While understanding the risk factors that are associated with an index HSI may be important for injury prevention, identification of risk factors associated with recurrent HSIs may be critical to the management of the index HSI as reinjuries are usually more severe with a longer time away from sport compared with the initial injury.[45] Older age and prior injury history are widely accepted risk factors for subsequent HSI.[50] Supporting evidence to predict

reinjury risk from MRI-based assessment immediately following HSI is equally mixed. Moderate evidence suggests reinjury risk may be associated with tissue-type and specific hamstring muscle involved in the index injury,[61] while more recent reviews have found that MRI descriptors of the index HSI do not accurately predict risk of reinjury.[50]

Although the mechanism linking prior injury with increased risk of reinjury is unclear, structural and functional deficits that are known to persist following an index HSI may play a role. Despite clinical decisions to determine readiness for RTS being based on the athlete's ability to demonstrate full range of motion, strength, and participation in asymptomatic sport-specific activities,[62] strength and morphological deficits are known to persist following HSI. At the time of RTS, between limb deficits of up to 10% on the previously injured limb or lower strength of injured athletes compared to uninjured athletes have been observed at the time of RTS.[63-66] Additional deficits known to persist following HSI include: reduced biceps femoris fascicle length,[41] biceps femoris atrophy,[65] and increased scar tissue.[67] Due to the known relationships between muscle structure and function,[68, 69] it is plausible that a relationship between known structural and strength deficits exists following HSI.

Known strength deficits at the time of RTS are thought to be linked to evidence of remaining injury observed on MRI.[65] While most studies[56, 65, 70, 71] quantify remaining injury based on MRI measures from fluid-sensitive sequences observed at the gross-anatomical level (e.g. length, cross sectional area, volume of hyperintensity), more recent studies[72, 73] have begun to explore evidence of remaining injury at RTS by investigating qualitative changes at the tissue level, such as the absence or presence of tendon waviness or discontinuity,[72, 73] muscle fiber tears, or loss of muscle pennation angle.[72] Regardless, neither quantitative measures at the whole muscle level, nor qualitative assessment of involvement at the tissue-specific level have demonstrated clear relationships with clinical outcomes, such as reinjury, following HSI.[50] Additional work to further quantify microstructural changes of muscle following

HSI and associated functional outcomes such as time to RTS, eccentric strength, and reinjury status is warranted to provide improved guidance for the clinical management of HSI.

The implementation of DTI to monitor muscle microstructure following HSI may hold potential in explaining the relationship between the structural and functional deficits known to exist following this injury. Initial work in the field demonstrates that DTI is sensitive to detect differences in the injured limb following acute HSI and demonstrates resolution of microstructural differences throughout recovery.[18] This robust study collected DTI data on 41 professional and recreational athletes at TOI, 2-weeks after TOI, and at RTS. They took a unique approach to analyzing the location of injury by identifying the cross-sectional area with the greatest evidence of injury and analyzing only the tissue immediately adjacent to that site (15 mm above and 15 mm below). They found that this method was able to successfully detect between limb differences in hamstring muscle microstructure at the TOI (MD, RD, λ_1, λ_2, λ_3) that were still present 2 weeks after injury (MD, λ_1, λ_2) but had resolved by RTS.[18] The association of these observations with clinical outcomes including time to RTS, muscle function, and reinjury status has not been previously explored.

Recently, DTI has been used to demonstrate an association with functional outcomes such as strength[74] and power[75, 76] in healthy individuals. Positive associations in diffusivity measures of muscles of the low back were identified with strength for all diffusivity measures (MD, RD, λ_1, λ_2, λ_3).[74] In the soleus, positive associations have been observed between maximum ankle power and FA and RD[75] and MD, λ_1, λ_2.[76] While the direct relationship between hamstring strength and DTI derived parameters of muscle microstructure has not been explored, a recent analysis demonstrated that a 12-week targeted hamstring eccentric strengthening program was able to detect a significant increase in fascicle length associated with the given intervention.[77]

Innovation

Taken together, the potential exists for more advanced, quantitative MRI measures to effectively monitor muscle microstructure and function as it relates to clinical outcomes for a more accurate prognosis resulting in improved care following an HSI. Due to the high reinjury rates observed following this injury, there is a great demand for more sensitive markers to monitor muscle microstructure and improve prognosis in attempts to aid in the management of injury recovery. The validity of DTI metrics used to represent muscle microstructure has been established.[78, 79] However, the implementation of these methods in an injured population are limited and the clinical utility of these measures has not been extensively studied. Although HSI's are known to be multifactorial, [50] the focus of the present analysis was to address this research gap by focusing on the independent relationships between quantitative MRI-based characteristics of injury and clinical outcomes. The prominent innovation of this proposal is two-fold—first, the implementation of a rigorous and thorough assessment of MRI-based quantitative measures of muscle morphology and microstructure for a prospective, longitudinal dataset; second, is the integration of conventional MRI based measures of muscle morphology and novel measure of DTI derived muscle microstructure with clinical outcomes such as time to RTS, eccentric hamstring strength, and reinjury status.

Thesis Outline

In this proposal, we aim to explore the utility of imaging-based methods to address the following challenges: Implementation of a rigorous and thorough assessment of MRI-based quantitative measures of muscle morphology and microstructure following HSI at TOI and throughout recovery; and determine the association of quantitative morphology measures and microstructural observations (2.) at TOI with clinical outcomes including time to RTS and reinjury incidence, and (3.) at RTS with clinical outcomes including eccentric strength and

reinjury incidence following HSI. In accordance with the aforementioned aims of this work, this thesis is organized as follows:

- **Chapter 2:** Diffusion tensor imaging quantifies differences in skeletal muscle microstructure after acute hamstring strain injury and throughout recovery
- **Chapter 3:** Association of quantitative imaging measures in acute hamstring strain injuries and longitudinal clinical outcomes including time to return to sport and reinjury
- **Chapter 4:** Association of quantitative imaging measures at the time of return to sport following acute hamstring strain injury with eccentric hamstring strength and reinjury incidence
- **Chapter 5:** A final summary of this work and discussions on related future work

Chapter 2.

Diffusion tensor imaging quantifies differences in skeletal muscle microstructure after acute hamstring strain injury and throughout recovery in collegiate athletes

Christa M. Wille, Samuel A. Hurley, Elizabeth Schmida, Kenneth Lee, Richard Kijowski, Bryan C. Heiderscheit

Abstract

Objective: To identify the region of interest (ROI) to represent injury and observe between-limb diffusion tensor imaging (DTI) microstructural differences in muscle following hamstring strain injury (HSI)

Methods: Participants who sustained an HSI at a single institution from 2017-2020 prospectively underwent 3T-MRI of bilateral thighs using T1, T2, and diffusion-weighted imaging at time of injury (TOI), return to sport (RTS), and 12-weeks after RTS (12wks). ROIs were using the hyperintense region on a T2-weighted sequence: edema, focused edema, and primary muscle injured excluding edema (no edema). Linear mixed-effects models were used to compare diffusion parameters between ROIs and timepoints and limbs and timepoints.

Results: Twenty-four participants (twenty-nine HSIs) were included. A significant ROI-by-timepoint interaction was detected for all diffusivity measures. The edema and focused edema ROIs demonstrated increased diffusion at TOI compared to RTS for all diffusivity measures (p-values<0.006), except λ_1 (p-values=0.058-0.12), and compared to 12wks (p-values<0.02). In the no edema ROI, differences in diffusivity measures were not observed (p-values>0.82). At TOI, no edema ROI diffusivity measures were lower than the edema ROI (p-values<0.001) but not at RTS or 12wks (p-values>0.69). A significant limb-by-timepoint interaction was detected for all diffusivity measures with increased diffusion in the involved limb at TOI (p-values<0.001)

but not at RTS or 12wks (p-values>0.42). Significant differences in fractional anisotropy over time or between-limbs were not detected.

Conclusion: Hyperintensity on T2-weighted imaging used to define the injured region holds promise in describing muscle microstructure following HSI by demonstrating between-limb differences at TOI but not at follow-up timepoints.

Clinical Relevance: Between-limb differences in muscle microstructure at TOI and resolution of differences throughout recovery is consistent with changes expected due to acute HSI and structural healing expected throughout recovery and may provide distinct information from outcomes gathered using T2-weighted imaging alone.

Introduction

Magnetic resonance imaging (MRI) is routinely used in soft tissue injury management, with recent advancements in quantitative MRI applications, such as diffusion tensor imaging (DTI), gaining interest due to its potential to aid in earlier diagnosis, increase prognostic accuracy, or monitor tissue changes following injury.[4] Muscle strain injuries, specifically of the hamstrings, are common in athletes and complicated by high rates of reinjury and limited prognostic indicators.[51] While the utility of conventional MRI observations following HSIs is widely debated,[15, 55-58] implementation of DTI following HSIs has shown potential in monitoring microstructural changes[18] that may be useful in the management of HSIs.

In the presence of injury, the relationship between actual diffusion changes and the resultant diffusion tensor is complex, due in part to increased extracellular water associated with edema.[25] Despite this, certain structural quantities averaged over a region of interest (ROI) have been shown to serve as a proxy for changes in structural features in the presence of muscle injury in humans.[10, 18-20] Increased signal on a T2-weighed image is often used to define the ROI used to represent injured tissue; however, a consensus on the exact definition has not been reached. A region defined by manual segmentation of the entire volume of increased signal on a T2-weighted image has demonstrated microstructural changes following muscle injury.[20] Other approaches have used a more focused region anchored to the slice identified as the center of the muscle injury,[10, 18] while others have used a select 1 cm^2 region.[19] The implications of the injury ROI definition used across sequential timepoints also remains unclear. Thus, a more thorough understanding of how ROI definition influences observed changes in diffusion parameters following acute injury and over time is warranted.

The purpose of this longitudinal, observational study was twofold: 1.) to investigate the ROI definition used to represent the injured region at time of injury (TOI) and at follow-up timepoints (return to sport (RTS); 12-weeks after RTS (12wks)); and 2.) to investigate

differences in diffusion parameters between-limbs at TOI and at follow-up timepoints. We hypothesized a volume defined by increased signal on a T2-weighted image, and a more focused region, would demonstrate significant differences in DTI-derived measures of muscle microstructure. In addition, we hypothesized that between-limb differences in muscle microstructure would be apparent at TOI, but resolve at RTS and 12wks following acute HSI.

Methods

The data presented in this study were collected as part of a larger prospective cohort investigation of collegiate athletes who sustained an HSI at a single institution from September 9th, 2017 to March 13th, 2020. The study was approved by the University's Health Sciences Institutional Review Board, and participants provided written informed consent prior to enrollment.

Study Design

Collegiate athletes participating in football, soccer, and track, who sustained an HSI confirmed by sports medicine staff and identified on MRI by a musculoskeletal radiologist (KL, RK) were included. An HSI was diagnosed as sudden onset of posterior thigh pain during an athletic event resulting in the athlete not being able to participate for at least one practice or competition, and the presence of two or more of the following: palpable pain along the hamstring muscles, posterior thigh pain without radicular symptoms during a passive straight leg raise, and/or weakness or pain with resisted knee flexion.[62] Participants were excluded if the injury was diagnosed as a complete muscle rupture and/or avulsion injury, or if the injury happened >7 days prior to seeking medical attention. The presence of injury on T2-weighted sequences was identified as a region of architectural disruption and/or hyperintense signal

within the hamstrings, most likely representing injury associated edema. Participants were excluded from this analysis if they had contraindications MRI.

A standardized rehabilitation protocol was implemented by the teams' athletic trainer, and RTS was determined when medical clearance was obtained to resume all sport-related activities. RTS clearance was based on a combination of factors including minimal to no pain with hamstring palpation, full hamstring range-of-motion, and no apprehension with on-field sports-specific movements. Repeat MRI examination was completed within 7 days of RTS and 12wks.

Magnetic Resonance Imaging Protocol

Participants received an MRI examination of bilateral thighs on a 3.0T scanner (GE Healthcare Discovery MR750, Waukesha, WI) using a 32-channel full torso coil and in a feet-first supine position. A 3D axial T1-weighted spoiled gradient recalled echo (SPGR) sequence was used for anatomical reference with the following parameters: no fat saturation, TR/TE=5.9/2.1 ms, flip=15°, FOV=44 cm, matrix=640x640 (reconstructed at 1024x1024), 80 slices, 5 mm thick, bandwidth=195 Hz/pixel, PURE intensity correction. A T2-weighted fast relaxation fast spin-echo sequence was used to identify region of injury with the following parameters: fat/water separation with iterative decomposition of water and fat with echo asymmetry and least-squares estimation (IDEAL), TR/TE=4,473/85.0 ms, matrix=448x448 (reconstructed to 512x512), 44 slices, 7 mm thick, 2 mm spacing, bandwidth=140 Hz/pixel. Diffusion-weighted images were acquired in two slabs using spin-echo echo planer imaging with weighting in 30 uniformly distributed directions on a unit sphere, 6 non-diffusion-weighted volumes (b=0 images), b-value of 500 s/mm^2, and other parameters: TR/TE=5770/51.1 ms, FOV=48 cm, matrix=160x160, 72 slices, 3 mm thick. The diffusion acquisition was repeated

twice with reversed phase-encode directions (anterior-posterior and posterior-anterior) to correct for susceptibility-induced distortions.

Magnetic Resonance Imaging Analysis

Clinical interpretations were performed by one of two musculoskeletal radiologists (RK, KL) each with over 20 years of experience. The primary muscle of injury was identified and the British Athletic Muscle Injury Classification (BAMIC)[6] scoring was completed using T1- and T2-weighted sequences.

For diffusion-weighted data, distortion, eddy current, and motion correction were performed using FSL TOPUP[33] and EDDY[34] and filtered using a local principal component analysis filter.[35] When small misalignments between T1- and diffusion-weighted scans occurred, they were manually registered by visually confirming all features were visible and aligned (skin/bone/muscle boundaries). Quantitative scalar measures analyzed from DTI images included fractional anisotropy (FA), mean diffusivity (MD), radial diffusivity (RD), and principal effective diffusivity eigenvalues (λ_1, λ_2, λ_3) and were calculated using FMRIB's Diffusion Toolbox (FMRIB Software Library, Oxford, UK).[80]

Region of Interest Analysis

Anatomical three-dimensional contours of each hamstring muscle (biceps femoris short head, biceps femoris long head, semitendinosus, semimembranosus) were completed via manual segmentation using T1-weighted axial SPGR images and ROIs defining the region of injury were created with manual identification of the hyperintense region on the axial T2-weighted fat/water separated IDEAL sequence (FSLeyes, v1.5.0, Oxford, UK).[81]

To better understand the influence of diffusion changes by ROI definition, three different ROIs were created: 1.) manual identification of the region of edema (edema), 2.) a more focused ROI within the region of edema (focused edema), and 3.) an ROI of the primary muscle injured, excluding the region of edema (no edema) (**Figure 2.1**). Musculoskeletal radiologists (KL, RK) identified the region of injury and manual segmentation was used to identify all voxels within this region. ROIs were further refined by taking the intersection of the muscle boundaries and the representative edema region and down-sampled to match the resolution of diffusion-weighted images. Morphological operations to erode one boundary pixel were completed to create the focused edema ROI. The no edema ROI was identified by subtracting the edema ROI from the primary injured muscle boundary.

Masks representing all ROIs were superimposed over the FA, MD, RD, and principal effective diffusivity eigenvalue maps to measure mean values of DTI measures within each area of interest (MATLAB, v2021b, Mathworks, Natick, MA). For between-limb comparisons, the edema ROI identified on the involved limb was mirrored and manually registered to the equivalent location on the uninvolved limb.

All muscle boundaries were manually created at each timepoint. Injury ROIs from TOI were registered to each subsequent timepoint using a 12 degree-of-freedom affine registration[82] performed on each limb individually (FSL, FMRIB Software Library, Oxford, UK). The estimated transform was applied to each ROI and manually adjusted as needed (**Figure 2.2A**).

A reliability assessment from eight healthy participants with no prior history of HSI was used to assess manual segmentation similarity between examiners and test-retest reliability of DTI parameters (**Supplemental Material 2.A**).

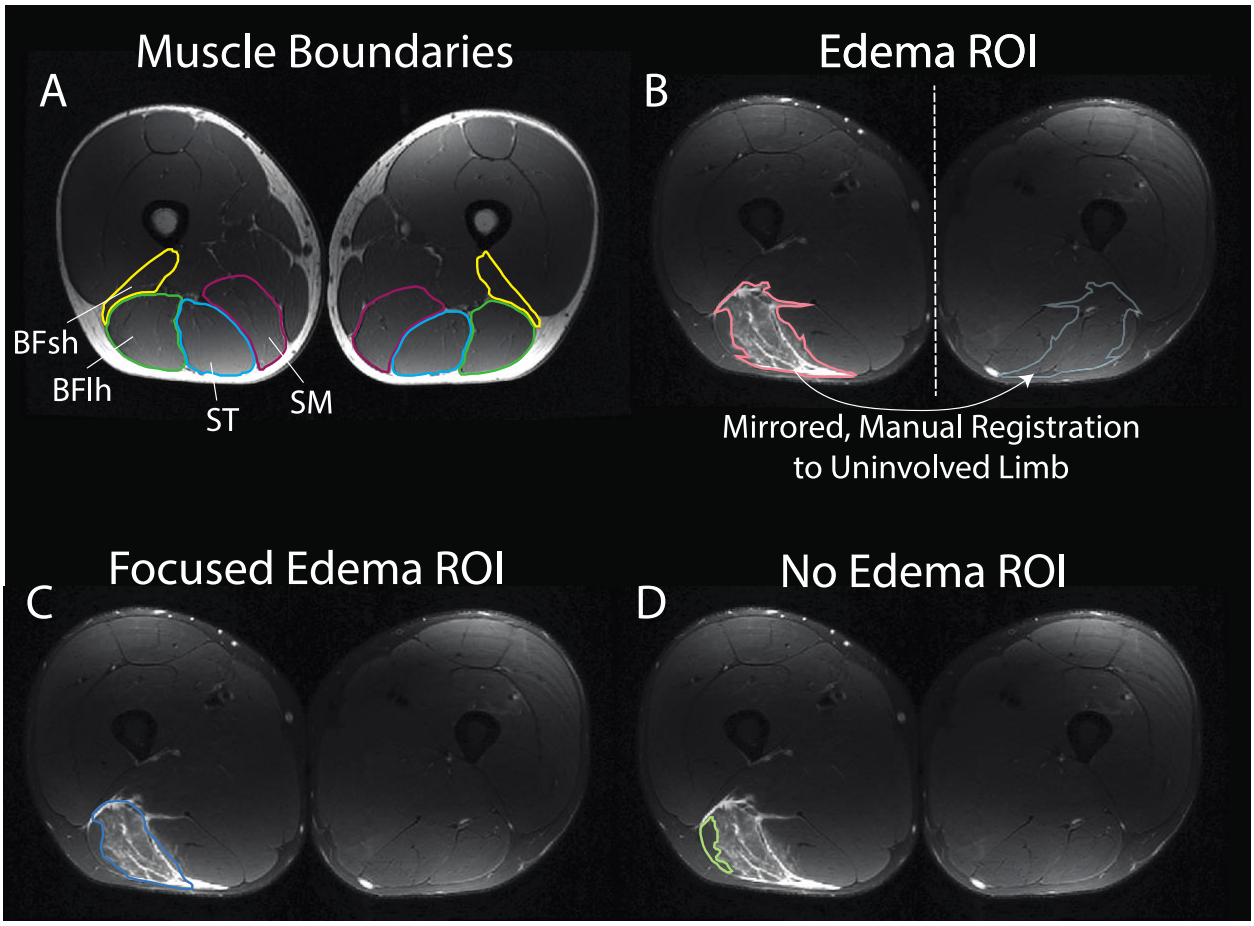

Figure 2.1. Mean quantitative diffusion metrics were calculated within manually outlined regions of interest (ROI) on the injured limb defined as A.) muscle boundary, B.) edema, C.) focused edema, and D.) primary injured muscle excluding the edema region. For between limb comparisons, ROIs were mirrored and manually registered to the uninvolved limb. Data shown are from one slice of a representative participant. Biceps femoris short head (BFsh), biceps femoris long head (BFlh), semitendinosus (ST), semimembranosus (SM).

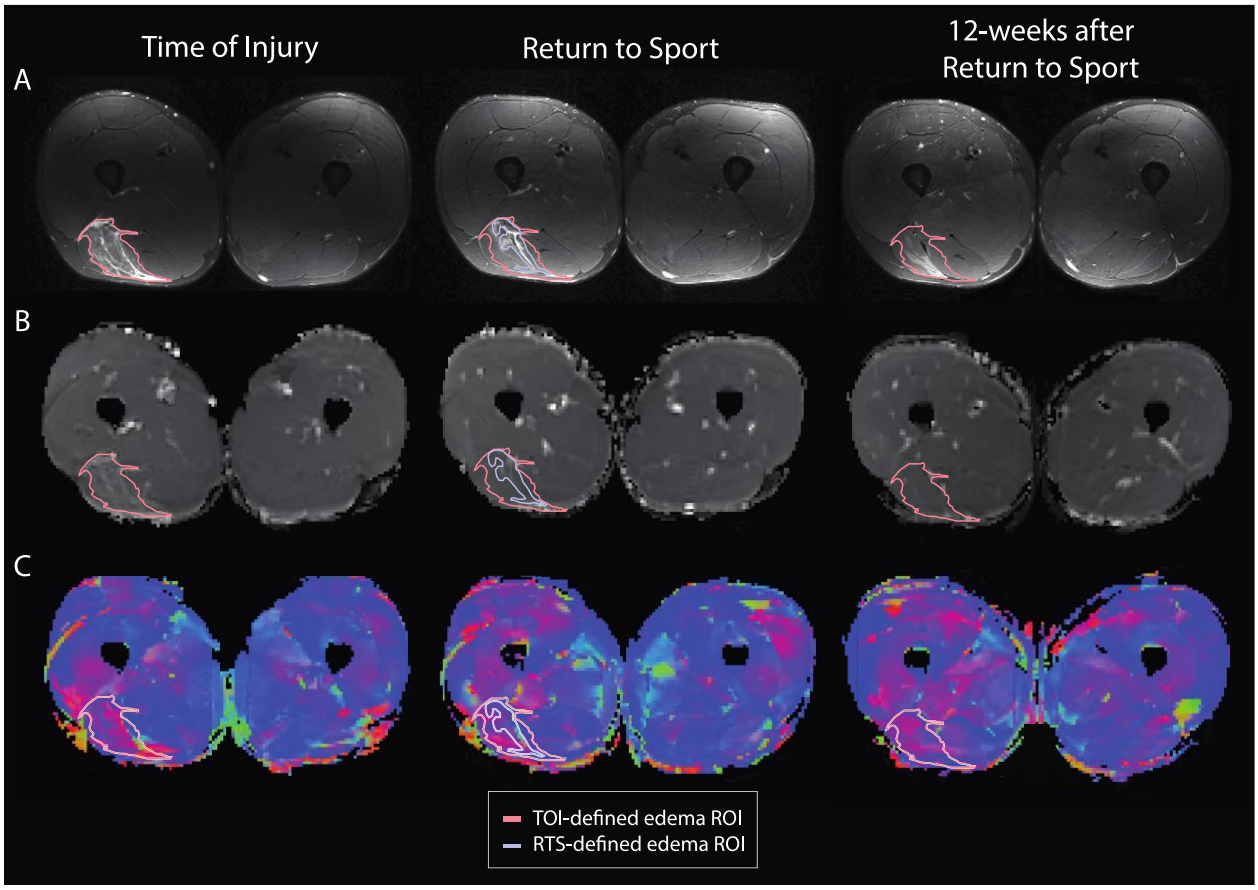

Figure 2.2. Representative imaging data from one participant at time of injury (TOI), return to sport (RTS), and 12 weeks after RTS; **A**.) T2-weighted, **B**.) mean diffusivity, and **C**.) primary eigenvalue maps along principal direction. Manually defined edema mask at TOI (peach) was registered to follow up scans to ensure a consistent region was compared across timepoints. Manually identified edema ROI mask at RTS (blue) used in Supplemental Material B.

Statistical Analysis

Standard descriptive statistics (mean/standard deviation, median/interquartile range, frequency/percentage) were used to describe the participants. Two sets of linear mixed-effects models were used to understand how 1.) ROI definition (edema, focused edema, no edema) and timepoint (TOI, RTS, 12wks) and 2.) limb (involved, uninvolved) and timepoint, and a potential interaction effect in each respective model, influenced diffusion parameters (FA, MD, RD, λ_1, λ_2, λ_3). In the ROI and timepoint models, only participant was assigned as a random effect. In the limb and timepoint models, the edema ROI at TOI and the TOI-registered edema

masks at RTS and 12wks were used to define the injured region. In this model, participant and limb were assigned as random effects. For variables with detected significant interaction, Tukey-adjusted *p*-values were used for pairwise comparisons between TOI and follow-up timepoints for each ROI or each limb separately. Least-square mean differences and associated confidence intervals (CI) are reported. All analyses were conducted using SAS v9.4 (SAS Institutes, Cary, NC) and significance was assessed at $\alpha \leq 0.05$.

Results

Twenty-four unique athletes met eligibility criteria, with 29 recorded HSIs (**Figure 2.3)**. The biceps femoris long head was the primary muscle most commonly injured (n=21). The median days to RTS was 21 (interquartile range 14-29). All participants at TOI (n=27) and RTS (n=18) had evidence of injury on T2-weighted sequences, while 50% (n=4/8) had evidence of injury at 12wks (**Table 2.1**).

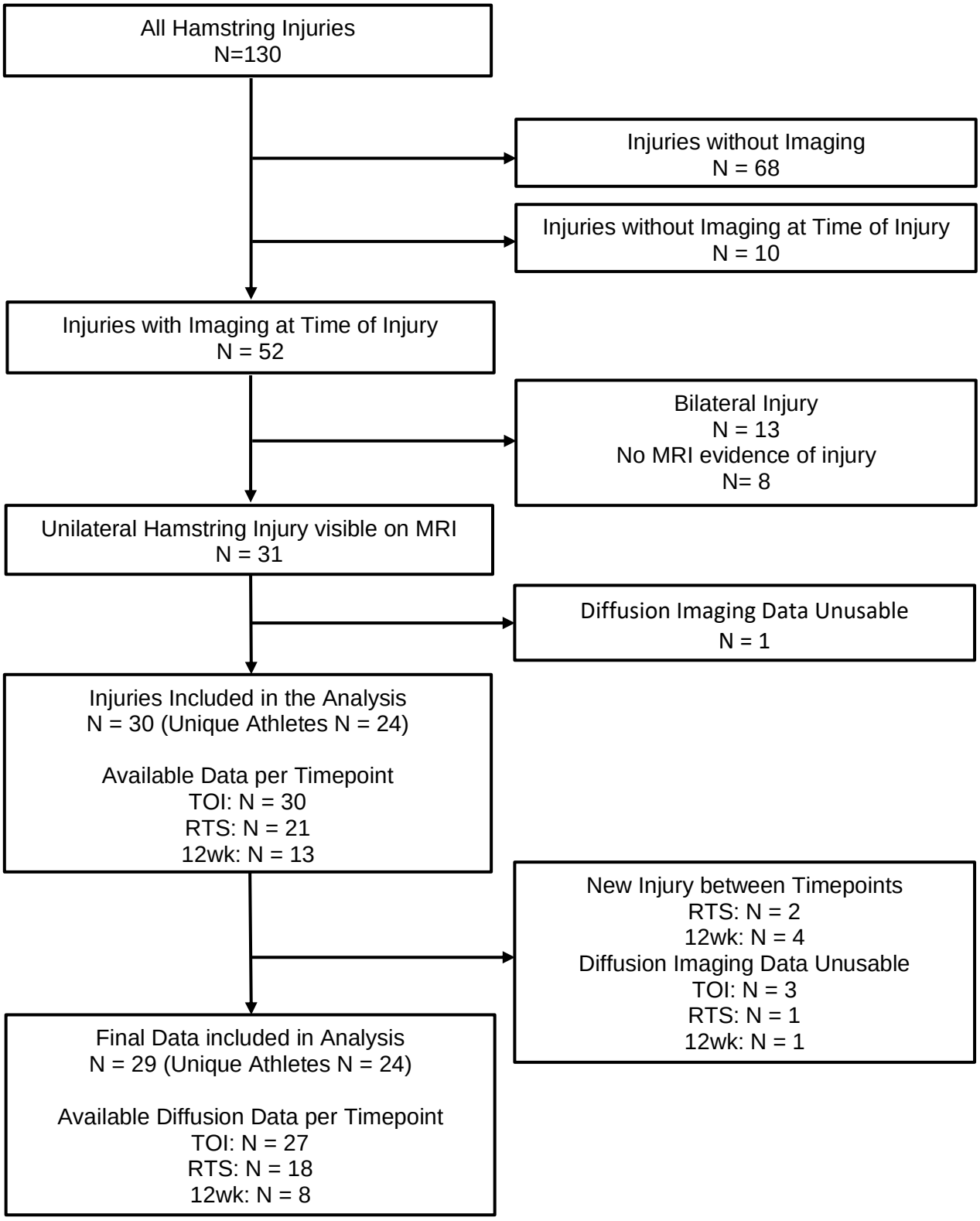

Figure 2.3. Participant inclusion criteria. All athletes included in this analysis had unilateral evidence of injury on a T2-weighted magnetic resonance image within 7 days of injury. Participants were excluded if reinjured or developed an additional injury between timepoints.

Table 2.1. Participant characteristics (n =24) and injury descriptions for all injuries (n = 29). Descriptive statistics related to edema presence are reported on data collected for all injuries at each timepoint: time of injury (TOI; n = 27); return to sport (RTS; n = 18); 12-weeks after RTS (12wks; n = 8). Edema presence is identified in participants with confirmed hyperintense signal in the hamstrings. Mean (standard deviation) of the manually identified volume of hyperintense signal on an axial T2-weighted sequence at each timepoint is reported.

Participant Characteristics		
		Mean (Standard Deviation)
Age (years)		19.8 (1.3)
Weight (kg)		86.5 (16.9)
Height (m)		1.83 (0.07)
		Count (%)
Females		3 (14.3)
Sport		
Football		11 (52.4)
Soccer		1 (4.8)
Track		12 (57.1)
Injury Descriptions		
British Athletic Muscle Injury Classification		**Count (%)**
1a		4 (15.4)
1b		3 (11.5)
2a		5 (19.2)
2b		3 (11.5)
2c		2 (7.7)
3a		1 (3.9)
3b		2 (7.7)
3c		9 (34.6)
Primary Muscle Injured		
Biceps Femoris Short Head		1 (3.9)
Biceps Femoris Long Head		21 (80.8)
Semitendinosus		3 (11.5)
Semimembranosus		4 (15.4)
Days to Return to Sport (Median, Interquartile Range)		21 (14-29)
Edema Presence by Timepoint	**Count (%)**	**Volume (cm^3)**
TOI	27 (100%)	80.2 (103.9)
RTS	18 (100%)	28.6 (50.1)
12wks	4 (50%)	70.0 (88.7)

Influence of Region of Injury Definition and Timepoint on Diffusion Parameters

A significant ROI-by-timepoint interaction term was detected for MD, RD, λ_1, λ_2, and λ_3 (*p*-values<0.006). Post-hoc pairwise testing to assess the influence of timepoint within the edema and focused edema ROI demonstrated a significant decrease in all diffusivity parameters from TOI to RTS, except λ_1 (edema: *p*=0.12; focused edema: *p*=0.058), and from TOI to 12wks, but not the no edema ROI (TOI to RTS: *p*-values=0.82-0.99; TOI to 12wks: *p*-values=0.99) (**Figure 2.4, Table 2.2**). Post-hoc pairwise testing to assess differences across ROIs within timepoint denoted significant differences at TOI for all diffusivity measures between the edema and no edema ROIs (p-values<0.001), with increased diffusivity in the edema ROI, while differences in diffusivity measures between the edema and focused edema ROIs were not detected (*p*-values>0.31). At RTS and 12wks, significant differences were not detected across any of the ROIs (*p*-values=0.69–0.99) (**Table 2.3**). For FA values, a significant ROI-by-time interaction term (*p*=0.38) was not detected. After removing the interaction term, neither the main effect for ROI (*p*=0.17), nor timepoint (*p*=0.09) were significant.

Influence of Limb and Timepoint on Diffusion Parameters

A significant limb-by-timepoint interaction term was detected for MD, RD, λ_1, λ_2, and λ_3 (*p*-values<0.004) **(Figure 2.5)**. Post-hoc pairwise comparisons denote a significant decrease over time for all diffusivity parameters of the injured region on the involved limb between TOI and RTS (*p*-values<0.03) and between TOI and 12wks (*p*-values<0.008). Significant changes over time were not detected on the uninvolved limb in any diffusivity parameters (*p*-values=0.63-0.99) (**Table 2.4**). Significant differences between-limbs were observed at TOI, with the involved limb showing increased diffusion in all diffusivity parameters (*p*-values<0.001). Significant between-limb differences at RTS and 12wks were not detected (*p*-values=0.42-0.99) (**Table**

2.5). For FA values, a significant limb-by-time interaction term (p=0.39) was not detected. After removing the interaction term, main effects for limb (p=0.84) or timepoint (p=0.12) were not detected.

An analysis using the edema, focused edema, and no edema ROIs identified from the hyperintense region present on respective T2-weighted images at TOI and RTS can be found in **Supplemental Material 2.B**.

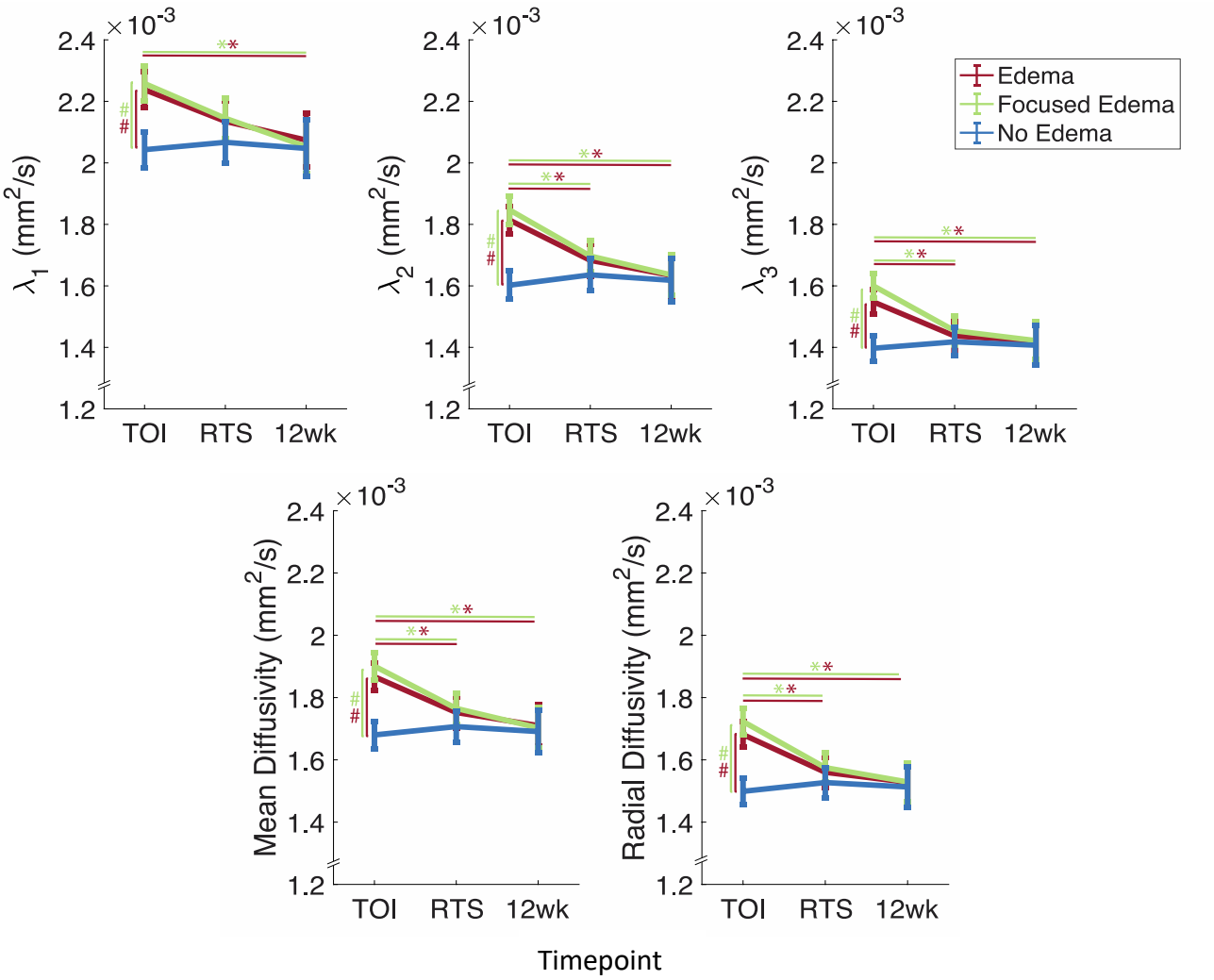

Figure 2.4. Least-square mean values for diffusion parameters within each region of interest (ROI: edema, focused edema, no edema) used to represent muscle injury. Error bars depict the 95% confidence intervals. Significant pairwise comparisons are denoted by # for ROI comparisons at each timepoint and * for timepoint comparisons within an ROI. Time of injury (TOI); Return to sport (RTS); 12-weeks after RTS (12wks).

Table 2.2. Diffusivity parameter least-square mean values mean differences [95% confidence intervals (CI)] from time of injury (TOI) and Tukey adjusted p-values for each region of interest at all timepoints (TOI, return to sport (RTS), and 12-weeks after RTS). A negative mean difference value denotes a decrease in the parameter compared to TOI. All diffusivity parameter values are reported in $mm^2/s*10^{-3}$. Mean diffusivity (MD); radial diffusivity (RD); principal effective diffusivity eigenvalues λ_1, λ_2, and λ_3.

		Return to Sport		12-weeks after RTS	
Variable	**Region of Interest**	**Mean Difference from TOI**	**p-Value**	**Mean Difference from TOI**	**p-Value**
MD	Edema	-0.11 [-0.20, -0.03]	0.002	-0.16 [-0.27, -0.05]	0.001
	Focused Edema	-0.14 [-0.22, -0.05]	<0.001	-0.20 [-0.31, -0.09]	<0.001
	No Edema	0.03 [-0.06, 0.11]	0.98	0.01 [-0.10, 0.12]	0.99
RD	Edema	-0.12 [-0.20, -0.04]	<0.001	-0.15 [-0.26, -0.05]	0.001
	Focused Edema	-0.15 [-0.26, -0.05]	0.001	-0.19 [-0.30, -0.09]	<0.001
	No Edema	0.03 [-0.05, 0.11]	0.97	0.01 [-0.10, 0.12]	0.99
λ_1	Edema	-0.10 [-0.22, 0.01]	0.12	-0.16 [-0.31, -0.01]	0.02
	Focused Edema	-0.11 [-0.23, 0.00]	0.058	-0.21 [-0.36, -0.06]	0.002
	No Edema	0.06 [-0.09, 0.14]	0.82	0.04 [-0.15, 0.16]	0.99
λ_2	Edema	-0.13 [-0.22, -0.04]	<0.001	-0.18 [-0.29, -0.07]	<0.001
	Focused Edema	-0.15 [-0.24, -0.06]	<0.001	-0.21 [-0.32, -0.10]	<0.001
	No Edema	0.03 [-0.05, 0.12]	0.93	0.02 [-0.10, 0.13]	0.99
λ_3	Edema	-0.11 [-0.19, -0.03]	0.001	-0.13 [-0.23, -0.02]	0.007
	Focused Edema	-0.15 [-0.23, -0.07]	<0.001	-0.18 [-0.28, -0.07]	<0.001
	No Edema	0.02 [-0.06, 0.10]	0.99	0.01 [-0.10, 0.12]	0.99

Table 2.3. Least square mean differences [95% confidence intervals] and Tukey adjusted p-values (edema region of interest (ROI) as reference) at all timepoints (time of injury, return to sport, and 12-weeks after return to sport). A negative mean difference value denotes a decrease in the parameter compared to the edema ROI. All diffusivity parameter values are reported in $mm^2/s*10^{-3}$. Mean diffusivity (MD); radial diffusivity (RD); principal effective diffusivity eigenvalues, λ_1, λ_2, and λ_3.

		Time of Injury		Return to Sport		12-weeks after RTS	
	Region of Interest	**Mean Difference from Edema ROI**	**p-Value**	**Mean Difference from Edema ROI**	**p-Value**	**Mean Difference from Edema ROI**	**p-Value**
MD	Focused	0.04 [-0.04, 0.11]	0.83	0.01 [-0.08, 0.10]	0.99	-0.01 [-0.13, 0.12]	0.99
	No Edema	-0.19 [-0.26, -0.11]	<0.001	-0.04 [-0.13, 0.05]	0.79	-0.02 [-0.15, 0.11]	0.99
RD	Focused	0.04 [-0.03, 0.11]	0.59	0.02 [-0.07, 0.10]	0.99	0.00 [-0.12, 0.12]	0.99
	No Edema	-0.18 [-0.25, -0.11]	<0.001	-0.03 [-0.12, 0.05]	0.94	-0.02 [-0.14, 0.11]	0.99
λ_1	Focused	0.02 [-0.08, 0.12]	0.99	0.01 [-0.11, 0.13]	0.99	-0.02 [-0.20, 0.15]	0.99
	No Edema	-0.20 [-0.30, -0.09]	<0.001	-0.07 [-0.19, 0.06]	0.69	-0.03 [-0.21, 0.16]	0.99
λ_2	Focused	0.03 [-0.04, 0.11]	0.89	0.01 [-0.08, 0.11]	0.99	0.00 [-0.13, 0.13]	0.99
	No Edema	-0.21 [-0.29, -0.14]	<0.001	-0.05 [-0.14, 0.05]	0.76	-0.02 [-0.15, -0.12]	0.99
λ_3	Focused	0.05 [-0.02, 0.12]	0.31	0.02 [-0.07, 0.10]	0.99	0.00 [-0.12, 0.12]	0.99
	No Edema	-0.15 [-0.22, 0.08]	<0.001	-0.02 [-0.10, 0.07]	0.99	-0.01 [-0.14, 0.11]	0.99

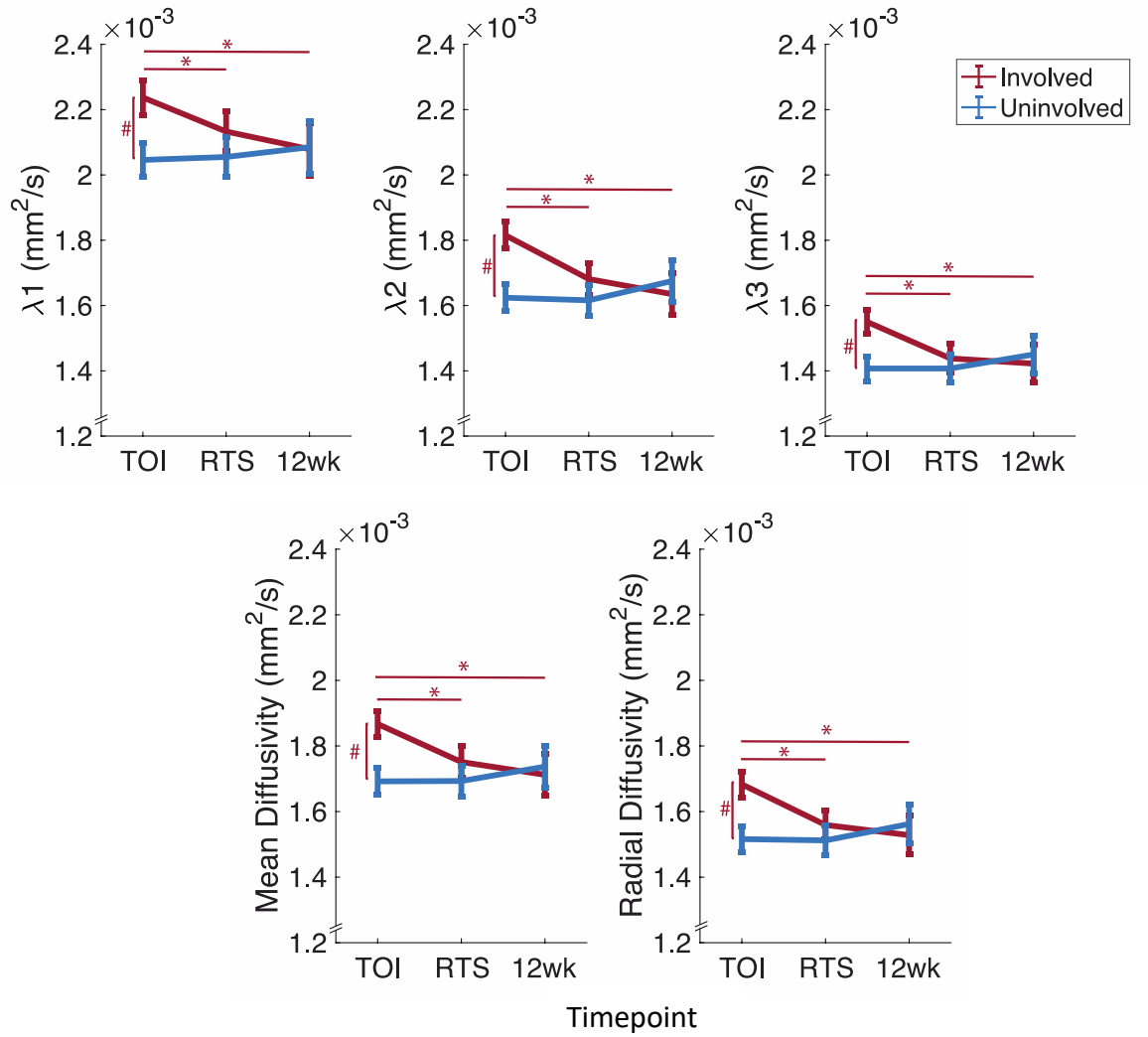

Figure 2.5. Least-square mean values for diffusion parameters within the edema region of interest defined at time on injury (TOI) on the involved limb and a mirrored region manually registered to the uninvolved limb. Error bars depict the 95% confidence intervals of the least-square mean. Significant pairwise comparisons are denoted by # for involved to uninvolved comparison within timepoints and * for within limb comparisons across timepoints. Time of injury (TOI); Return to sport (RTS); 12-weeks after RTS (12wks).

Table 2.4. Diffusivity parameter mean differences [95% confidence intervals (CI)] from time of injury (TOI) and Tukey adjusted p-values for involved and uninvolved limb diffusivity parameters within the edema region of interest at all timepoints (TOI, return to sport (RTS), 12-weeks after RTS). A negative value denotes a decrease in the parameter compared to the time of injury. All diffusivity parameter values were averaged within the edema region of interest defined at TOI and are reported in $mm^2/s*10^{-3}$. Mean diffusivity (MD); radial diffusivity (RD); principal effective diffusivity eigenvalues, λ_1, λ_2, and λ_3.

		Return to Sport		12-weeks after RTS	
Variable	**Limb**	**Mean Difference From TOI**	**p-Value**	**Mean Difference from TOI**	**p-Value**
MD	Involved	-0.12 [-0.19, -0.04]	<0.001	-0.16 [-0.25, -0.06]	<0.001
	Uninvolved	0.00 [-0.07, 0.07]	0.99	0.04 [-0.05, 0.14]	0.75
RD	Involved	-0.12 [-0.19, -0.05]	<0.001	-0.15 [-0.25, -0.06]	<0.001
	Uninvolved	0.00 [-0.07, 0.07]	0.99	0.05 [-0.04, 0.14]	0.65
λ_1	Involved	-0.10 [-0.20, -0.01]	0.03	-0.16 [-0.28, -0.03]	0.008
	Uninvolved	0.01 [-0.09, 0.11]	0.99	0.04 [-0.09, 0.17]	0.94
λ_2	Involved	-0.13 [-0.21, -0.06]	<0.001	-0.18 [-0.28, -0.08]	<0.001
	Uninvolved	-0.01 [-0.08, 0.07]	0.99	0.05 [-0.05, 0.15]	0.63
λ_3	Involved	-0.11 [-0.18, -0.04]	<0.001	-0.13 [-0.22, -0.04]	<0.001
	Uninvolved	0.00 [-0.07, 0.07]	0.99	0.04 [-0.05, 0.13]	0.71

Table 2.5. Between limb differences of least square mean values [95% confidence intervals] of diffusivity parameters within the edema region of interest defined at time of injury and Tukey adjusted p-values (uninvolved limb as reference) at all timepoints (time of injury, return to sport (RTS), 12-weeks after RTS). A negative value denotes a decrease in the parameter compared to the uninvolved limb. All diffusivity parameter values are reported in $mm^2/s*10^{-3}$. Mean diffusivity (MD); radial diffusivity (RD); principal effective diffusivity eigenvalues, λ_1, λ_2, and λ_3.

	Time of Injury		Return to Sport		12-weeks after RTS	
	Between Limb Mean Difference	**p-Value**	**Between Limb Mean Difference**	**p-Value**	**Between Limb Mean Difference**	**p-Value**
MD	0.18 [0.09, 0.26]	<0.001	0.06 [-0.04, 0.16]	0.51	-0.02 [-0.16, 0.11]	0.99
RD	0.17 [0.09, 0.25]	<0.001	0.05 [-0.05, 0.14]	0.66	-0.03 [-0.16, 0.09]	0.96
λ_1	0.19 [0.08, 0.30]	<0.001	0.08 [-0.05, 0.21]	0.46	-0.01 [-0.18, 0.17]	0.99
λ_2	0.19 [0.10, 0.28]	<0.001	0.06 [-0.04, 0.17]	0.42	-0.04 [-0.17, 0.09]	0.94
λ_3	0.14 [0.06, 0.22]	<0.001	0.03 [-0.06, 0.12]	0.91	-0.03 [-0.15, 0.09]	0.98

Discussion

The purpose of this study was to use DTI to quantify changes in skeletal muscle following HSI by investigating differences in quantitative diffusion parameters, first across different ROI definitions to represent the injured region, and second between limbs at TOI, RTS, and 12wks. In support of our hypothesis, edema and focused edema ROIs demonstrated increased diffusivity parameters (MD, RD, λ_1, λ_2, λ_3) compared to the no edema ROI at TOI. Using the edema ROI to represent the injured region, increased diffusivity parameters (MD, RD, λ_1, λ_2, λ_3) were only present at TOI in the involved limb compared to the uninvolved.

In the presence of injury, a decrease in the directional anisotropy (FA) and an increase in diffusivity measures (MD, RD, λ_1, λ_2, λ_3), consistent with less restricted diffusion, is expected. Findings from this study are consistent with previous literature assessing acute[19, 20] and longitudinal[10, 18] observations following musculoskeletal injury in humans with increased MD,[18, 20] RD,[18, 20] and eigenvalues (λ_1, λ_2, λ_3)[18, 19] in the injured region at TOI and significant reductions in MD and eigenvalues[10, 18] at RTS. Analyses in this study provide a more thorough assessment of the ROI used to represent the injured region and provide additional longitudinal data at 12wks from a larger, more homogenous sample, with injuries isolated to the hamstrings.

Despite good agreement between FA values in this study with published values from other studies of acute muscle injuries in humans,[10, 19, 20] neither a significant difference over time nor between-limbs was detected for FA. Similar results demonstrating expected changes in MD and eigenvalues, but not FA, have been previously reported.[18, 83, 84] Because FA is used to characterize the degree of difference among the eigenvalues, lack of significant findings may imply that comparable increases in the eigenvalues could resemble diffusion ellipsoids that change approximately equally along all axes. If the relative degree of difference among eigenvalues does not change, only the magnitudes, then a significant difference in FA will not

be observed. Although FA is a key outcome measure in diffusion-imaging of the brain, the impact of microstructural changes on FA in skeletal muscle may not be as strong as the impact on each of the individual eigenvalues due to the relative similarities in the axial versus radial diffusivities of muscle compared to brain.

Influence of Region of Injury Definition and Timepoint

When analyzing DTI data in the presence of muscle injury, current practices rely on edema to define the injured region, further complicating the relationship between the diffusion tensor and inferred measures of microstructure. In our analysis at TOI, a significant increase in diffusion parameters was observed in the edema and focused edema ROIs, but not detected in the no edema ROI. This indicates that either the presence of edema may be driving the diffusivity changes, or the location of edema reflects the area where microstructural changes are present. Although single-shell diffusion-weighted imaging with tensor fitting is unable to resolve the source of the observed signal changes, it is worth noting that similar findings were observed when analyzing diffusion changes at RTS regardless of whether the TOI-registered edema ROI was used or the ROI defined by the presence of edema at RTS (**Supplemental Material 2.B**). The notable change in average edema volume from TOI to RTS further supports this, as the respective ROIs will reflect a similar change. With a smaller volume and increased T2-weighted signal throughout, the RTS-defined edema ROIs contained a much larger volume fraction of edema compared to the TOI-registered edema ROIs. Because similar conclusions can be made using either ROI, it is likely that diffusion changes observed in this study are representative of microstructural changes consistent with healing and not solely driven by the presence of edema. Thus, an ROI defined by signal hyperintensity on a T2-weighted image at TOI and registered across follow-up timepoints may best represent the injured region and allow for a systematic comparison across longitudinal data.

Advantages of the ROIs investigated in this study include the objective approaches used relying on morphological operations to systematically erode boundary pixels to create the focused edema ROI and robust registration algorithms to systematically register ROIs across timepoints. While the idea of a focused region within the entire region of injury has been previously explored, subjective input to determine the greatest slice or exact location of injury was utilized in prior analyses and requires additional input to define ROIs over sequential timepoints.[10, 18] To our knowledge, the comparison of ROIs containing the entire region of edema alongside ROIs of a more focused region has not been previously done. While results from the edema and focused edema ROI were similar in this analysis, a marginally significant increase in λ_1 at TOI was detected using a focused edema ROI, not apparent in the edema ROI. The systematic morphological operations to erode one boundary pixel to create a more focused ROI may demonstrate a robust method for the identification of a focused region to represent injury. Further exploration of the benefits of the potential increased sensitivity of the focused edema ROI is warranted.

Influence of Limb and Timepoint

Quantitative DTI parameters consistent with injury in a volume defined by hyperintensity on a T2-weighted image were observed in the involved limb compared to the mirrored region on the uninvolved limb. Furthermore, diffusivity measures in the involved limb significantly decreased such that at RTS or 12wks there were no detectable differences between-limbs. The resolution of between-limb microstructural differences at follow-up timepoints may represent healing of the structural degradation in the injured region.

Initial evidence supports the use of DTI to characterize between-limb differences in muscle microstructure at TOI.[10, 19, 20] While, preliminary evidence indicates that DTI parameters demonstrate significant differences between TOI and RTS,[10, 18] differences in

study designs, such as ROI definitions[10, 18] and comparison of injuries across a heterogeneous sample of muscles,[10] limits the ability to draw definite conclusions. Additional information from this study further supports that between-limb differences in DTI parameters at TOI are no longer detected at RTS and 12wks following HSIs.

Despite the resolution of all clinical symptoms and the return to prior activity levels, continued evidence of injury on MRI at RTS has been discussed as a measure of incomplete recovery with a potential association to reinjury susceptibility.[56] Previous findings demonstrate persistent edema at RTS is common following acute HSI.[56, 65] Similarly, at RTS all participants in this study demonstrated increased signal hyperintensity on T2-weighted imaging, despite being cleared by their teams' medical staff, yet between-limb differences in microstructural measures were not present. Thus, quantitative measures of muscle microstructure identified with DTI may demonstrate a different relationship with injury prognosis or reinjury rates than information gathered from T2-weighted imaging.

Limitations

Total MRI acquisition time for this study was under 45-minutes and proved adequate to reveal subtle changes in DTI parameters of skeletal muscle. Advanced techniques such as more averaging or increased diffusion-gradient directions[28, 32] to increase signal-to-noise ratio or multi-shell diffusion imaging,[23-25] and multi-exponential T2 quantitative mapping[25] to improve the specificity of DTI to measure microstructural changes in the presence of injury may be advantageous. However, the clinical implementation of these techniques is limited by sequence optimization and protocol times when imaging a relatively large body segment such as the thighs. It is worth noting that although the sample-size at TOI is respectable (n=27), attrition at follow-up timepoints (RTS n=18, 12wks n=8) occurred due to scheduling conflicts and subsequent injuries, as expected with elite athletes. Although significant improvements in

diffusivity measures consistent with tissue healing were observed in this study, correlation of these findings to clinical outcome measures such as muscle function and reinjury is warranted.

Conclusion

The use of T2-weighted imaging at TOI to define the injured region, and registered to subsequent images, demonstrates promise in describing muscle microstructural changes associated with injury and throughout recovery. When using the edema ROI to define the injured region, between-limb differences in DTI-derived measures of muscle microstructure were detected at TOI but not at RTS and 12wks; likely demonstrating expected changes consistent with healing. Although the presence of edema complicates the interpretation of diffusion parameters, the resolution of between-limb differences in DTI-derived parameters despite continued edema at follow-up timepoints demonstrates diffusion-weighted imaging may provide distinct information from parameters derived from T2-weighted imaging alone. Future work is necessary to describe the relationship between DTI-derived measures of muscle microstructure and clinical outcomes such as muscle function, injury prognosis, or reinjury susceptibility.

Supplemental Material 2.A. Reliability Tests

Purpose

To assess (1.) the similarity of manual segmentation methods across examiners and (2.) test-retest reliability of diffusion tensor imaging (DTI) parameters within hamstring muscles in a healthy population.

Methods

Pilot data from eight healthy participants with no prior history of hamstring strain injury (HSI) were used. Each participant completed the imaging protocol twice, with repositioning between each set of sequences. Manual segmentation of each hamstring muscle (biceps femoris short head, BFsh; biceps femoris long head, BFlh; semitendinosus, ST; semimembranosus, SM) was completed using the unique T1-weighted sequences. While blinded to the assessment from the first examiner (CW), manual segmentations were performed by a second examiner (ES) on one T1-weighted sequence per subject to determine the similarity of manual segmentation methods across examiners. The muscle ROIs were converted to binary images and Sørensen-Dice similarity coefficient was used to determine the similarity of segmentations between examiners.

To assess the test-retest reliability of DTI parameters, manual segmentations were completed by the same examiner (ES) across both T1-weighted sequences specific to each test set of images. Manual segmentations were down sampled and overlaid with diffusion maps. When small misalignments between T1- and diffusion-weighted scans occurred, they were manually registered by visually confirming that all features were visible and aligned on all scans (skin/bone/muscle boundaries). DTI parameters of interest were averaged across each muscle group and compared within subjects, across repeated imaging sets. Intraclass correlation coefficients (ICCs) using a two-way mixed model to determine consistency (ICC(3,1))[85, 86]

were calculated for all diffusivity measures within each muscle group of interest and averaged across muscles. Standard error of measurement (SEM) was reported as $SEM = standard\ deviation * \sqrt{1 - ICC}$, where $standard\ deviation = \sqrt{sum\ of\ squares\ total/(n-1)}$. Minimal detectable change (MDC_{95}) was calculated as $MDC_{95} = SEM * 1.96 * \sqrt{2}$ and coefficients of variation (CV) were calculated as $CV = SEM/mean(trial\ 1, trial\ 2)$.[87] All analyses were performed using custom MATLAB algorithms (version 2021b, Mathworks, Natick, MA).

Results

Excellent similarity was achieved across examiners, dice similarity coefficient 0.917 $\pm$0.015. ICC values ranged from 0.59-0.82, SEM values ranged from 0.016-0.044, MDC_{95} ranged from 0.45-0.123, and CV ranged from (1.7-7.9%) (**Table 2.S1**).

Table 2.S1. Test-retest reliability of diffusion tensor imaging parameters in hamstring muscles. Intraclass correlation coefficient (ICC), 95% confidence interval [95% CI], coefficient of variation (CV), standard error of measurement (SEM), minimal detectable change with 95% confidence (MDC_{95}), fractional anisotropy (FA), mean diffusivity (MD), radial diffusivity (RD), and principal effective diffusivity eigenvalues λ_1, λ_2, λ_3).

	ICC [95% CI]	**SEM ($mm^2/s*10^{-3}$)$^+$**	**MDC_{95} ($mm^2/s*10^{-3}$)$^+$**	**CV**
FA	0.82 [0.57, 0.93]	0.016 [-]	0.045 [-]	7.9%
MD	0.65 [0.25, 0.86]	0.029	0.079	1.7%
RD	0.68 [0.34, 0.87]	0.044	0.123	2.2%
λ_1	0.59 [0.17, 0.83]	0.039	0.109	2.5%
λ_2	0.78 [0.49, 0.92]	0.033	0.090	2.3%
λ_3	0.65 [0.27, 0.86]	0.036	0.101	2.4%

$^+$SEM and MDC_{95} values are reported in $mm^2/s*10^{-3}$, except for FA values as indicated as unitless [-].

Supplemental Material 2.B. Region of injury defined by hyperintense signal at each timepoint

Purpose

To explore the influence of the injured region used at a sequential imaging time point as defined by (1.) the registered region of hyperintense signal at time of injury (TOI) or by (2.) manual segmentation of the hyperintense region present at return to sport (RTS).

Methods

Specific regions of interest (ROI) defining the region of injury were created with manual identification of the hyperintense region on the axial T2-weighted fat/water separated IDEAL sequence (FSLeyes, v1.5.0, Oxford, England) on the involved limb at TOI and RTS. The edema ROI identified on the involved limb was mirrored and manually registered to the equivalent location on the uninvolved limb at both time points. Injury ROIs from TOI were registered to RTS imaging using a 12 degree-of-freedom affine registration [82].

All ROIs contained only contractile muscle tissue, as defined by pixels with overlapping inclusion in both anatomical 3D contours of each hamstring muscle identified by manual segmentation on T1-weighted axial SPGR images. Masks representing all ROIs were superimposed over the fractional anisotropy (FA), mean diffusivity (MD), radial diffusivity (RD), and principal effective diffusivity eigenvalue maps λ_1, λ_2, λ_3 to measure the mean values of quantitative diffusion tensor imaging (DTI) outcome measures within each area of interest (MATLAB, v2021b, Mathworks, Natick, MA).

A paired t-test was used to compare diffusion parameters at RTS averaged over an ROI defined by the hyperintense region on a T2-weighted sequence at TOI and registered to RTS imaging data versus averaged diffusion data within the hyperintense region present at RTS. A linear mixed effect model was used to understand how limb and time point influenced

microstructural parameters when the injured region was defined by the hyperintense region on a T2-weighted sequence at each respective time point.

Results

No significant differences in averaged DTI-derived measures of muscle microstructure exist when comparing the injured region defined by the hyperintense region on a T2-weighted image at TOI registered to RTS data verses the region defined by the hyperintense region on a T2-weighted image at RTS (p-values = 0.20-0.59) (**Table 2.S2**).

When the injured region was defined by the hyperintense region on a T2-weighted sequence at each respective time point, a significant limb-by-timepoint interaction term was detected for MD (p=0.03), RD (p=0.05), λ_2 (p=0.04), and λ_3 (p= 0.02). Post-hoc pairwise comparisons denote significant differences between limbs at TOI, with the involved limb showing increased diffusion in MD, RD, λ_2, and λ_3 diffusivity parameters ($p < 0.01$). Significant differences between limbs at RTS were not detected in any diffusivity parameters (p = 0.14-0.89). Significant changes over time were observed for MD, RD, and λ_2 diffusivity parameters demonstrating a decrease in the diffusion overtime of the injured region on the involved limb (TOI to RTS: $p \leq 0.02$-0.03) but not for λ_2 (p=0.06). Significant changes over time were not detected on the uninvolved limb in any diffusivity parameters (p=0.79-0.99). For λ_1 values, a significant limb-by-time interaction term (p = 0.08) was not detected. After removing the interaction term, significant main effects were detected for limb (Least Square Means (95% CI), involved: 2.19 (2.14, 2.24), uninvolved: 2.05 (2.00, 2.10); $p < 0.01$) and timepoint (TOI: 2.13 (2.10, 2.18), RTS: 2.10 (2.05, 2.15); p = 0.04). (**Figure 2.S1, Table 2.S3 and 2.S4**). For FA values, a significant limb-by-time interaction term (p = 0.15) was not detected. After removing the interaction term, main effects for limb (p = 0.97) or timepoint (p = 0.94) were not detected.

Table 2.S2. Paired t-test results comparing mean differences [95% confidence intervals (CI)] in diffusivity parameters within the injured region defined by the hyperintense region on a T2-weighted image at TOI registered to RTS data verses the region defined by the hyperintense region on a T2-weighted image at RTS. A negative value denotes a decrease in the averaged parameters defined across the region based on hyperintensity at RTS compared to a region defined at TOI and registered to RTS data. All diffusivity parameter values are reported in $mm^2/s*10^{-3}$. Mean diffusivity (MD); radial diffusivity (RD); principal effective diffusivity eigenvalues λ_2, λ_2, and λ_3.

Parameter	Mean Difference [95% CI]	p-Value
FA	0.01 [-0.02, 0.03]	0.59
MD	-0.03 [-0.08, 0.02]	0.26
RD	-0.03 [-0.07, 0.02]	0.20
λ_1	-0.02 [-0.06, 0.03]	0.40
λ_2	-0.04 [-0.10, 0.03]	0.26
λ_3	-0.03 [-0.10, 0.04]	0.39

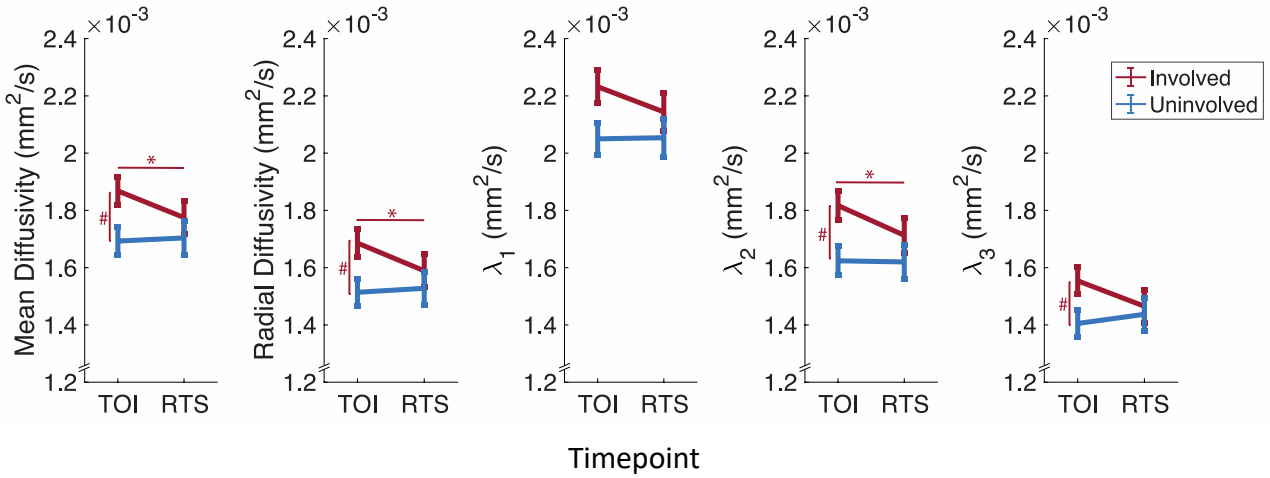

Figure 2.S1. Least-square mean values for diffusion parameters within the manually defined hyperintense region on T2-weighted image (edema region of interest) to represent muscle injury on the involved limb and a mirrored region manually registered to the uninvolved limb. Error bars depict the 95% confidence intervals of the least-square mean. Significant pairwise comparisons are denoted by # for involved to uninvolved comparison within timepoints and * for within limb comparisons across timepoints. Time of Injury (TOI), Return to Sport (RTS).

Table 2.S3. Diffusivity parameter least-square mean values [95% confidence intervals (CI)], mean differences from time of injury (TOI) and Tukey adjusted p-values for involved and uninvolved limb diffusivity parameters at all timepoints (TOI, return to sport). A negative value denotes a decrease in the parameter compared to TOI. All diffusivity parameter values are reported in $mm^2/s*10^{-3}$. Mean diffusivity (MD); radial diffusivity (RD); principal effective diffusivity eigenvalues λ_2, and λ_3.

		Return to Sport	
Variable	**Limb**	**Mean Difference from TOI**	**p-Value**
MD	Involved	-0.09 [-0.18, -0.01]	0.03
	Uninvolved	0.01 [-0.08, 0.10]	0.99
RD	Involved	-0.10 [-0.18, -0.01]	0.03
	Uninvolved	0.01 [-0.08, 0.10]	0.98
λ_2	Involved	-0.10 [-0.19, -0.01]	0.02
	Uninvolved	0.00 [-0.09, 0.09]	0.99
λ_3	Involved	-0.09 [-0.18, 0.00]	0.06
	Uninvolved	0.03 [-0.06, 0.12]	0.79

Table 2.S4. Between limb differences of least square means [95% confidence intervals] and Tukey adjusted p-values (uninvolved limb as reference) at time of injury and return to sport. Mean diffusivity (MD); radial diffusivity (RD); principal effective diffusivity eigenvalues λ_2, and λ_3.

	Time of Injury		Return to Sport	
Variable	**Between Limb Mean Difference**	**p-Value**	**Between Limb Mean Difference**	**p-Value**
MD	0.18 [0.08, 0.27]	<0.001	0.07 [-0.04, 0.18]	0.30
RD	0.17 [0.08, 0.26]	<0.001	0.06 [-0.05, 0.17]	0.43
λ_2	0.19 [0.10, 0.29]	<0.001	0.09 [-0.02, 0.21]	0.14
λ_3	0.15 [-0.06, 0.24]	0.001	0.03 [-0.08, 0.14]	0.89

Chapter 3.

Association of quantitative imaging measures in acute hamstring strain injuries and longitudinal clinical outcomes including time to return to sport and reinjury incidence

Christa M. Wille, Samuel A. Hurley, Mikel R. Stiffler-Joachim, Kenneth Lee, Richard Kijowski, Bryan C. Heiderscheit

Abstract

Hamstring strain injuries (HSI) are a common occurrence in athletics and complicated by limited prognostic indicators and high rates of reinjury. Assessment of injury characteristics at the time of injury (TOI) may be used to manage athlete expectations for the time to return to sport (RTS) and mitigate reinjury risk. Magnetic resonance imaging (MRI) is routinely used in soft tissue injury management, but its prognostic value for HSI is widely debated. Recent advancements in musculoskeletal MRI, such as diffusion tensor imaging (DTI), have allowed for additional quantitative measures of muscle microstructure assessment. The purpose of this study was to determine the association of TOI MRI-based measures, including the British Athletic Muscle Injury Classification (BAMIC) system, and quantitative imaging measures, such as edema volume and DTI metrics, with time to RTS and reinjury incidence. Negative binomial regressions and generalized estimating equations were used to determine relationships between imaging measures and time to RTS and reinjury status, respectively. Twenty-six injuries were observed, with five recorded reinjuries. BAMIC score and edema volume at TOI were not associated with days to RTS (p-values $\geq$ 0.15) or reinjury (p-values $\geq$ 0.13). A significant association between DTI metrics and days to RTS was not detected (p-values $\geq$ 0.11). Decreased diffusivity metrics were observed in those who reinjured (mean diffusivity, p = 0.016; radial diffusivity, p = 0.02; principal effective diffusivity eigenvalues, p-values = 0.007-0.057). Additional work to further understand the directional relationship observed between DTI metrics and reinjury status and the influence of external factors is warranted.

Introduction

Muscle strain injuries, specifically of the hamstrings, are a common occurrence in athletics and complicated by limited prognostic indicators and high rates of reinjury.[51, 52] Hamstring strain injuries (HSI) result in significant loss of time from activity, decreased quality of life,[48] and increased financial burden in elite sports.[49] Accurate prediction of the recovery time needed to return to sport (RTS) based on injury characteristics at the time of injury (TOI) has considerable value in managing athlete expectations, guiding activity progression, and mitigating reinjury risk.

Magnetic resonance imaging (MRI) is routinely used to aid in soft tissue injury management and prognosis in a sports medicine setting.[3] However, the prognostic value of MRI-based assessments within days following an acute HSI is widely debated.[15, 55-58] The majority of these assessments are at the gross anatomical level (i.e., volume, location, number of muscles involved),[58] and do not appear to improve predicting time to RTS beyond physical examination metrics and athlete HSI history.[15, 59] Conversely, there is a growing body of evidence supporting the association between MRI-based injury grading scales, such as the British Athletics Muscle Injury Classification (BAMIC), and time to RTS.[10-12, 14, 60] Results on predicting reinjury risk from MRI assessment following HSI are equally mixed. Moderate evidence suggests reinjury risk is associated with the hamstring muscle or the tissue-type involved in the index injury,[61] while others have found that MRI descriptors of the index HSI do not accurately predict risk of reinjury.[50]

Recent advancements in musculoskeletal MRI such as diffusion tensor imaging (DTI) have allowed for additional quantitative measures of muscle microstructure at the cellular level. DTI generates contrast from the random diffusion of water molecules, and utilizes differences in diffusivity to infer information about muscle microstructure. The microstructure of an intact muscle fiber will encourage water to preferentially diffuse along the direction of the fiber, while diffusion will occur in a more random and directionally isotropic pattern in injured or damaged

muscle fibers.[22] Preliminary evidence demonstrates that DTI is sensitive to detect differences in the injured limb following acute HSI.[18] However, the association of DTI parameters following acute HSI and longitudinal clinical outcomes such as time to RTS and reinjury incidence has not yet been explored.

Therefore, the purpose of this study was to determine the association of MRI-based injury grading and quantitative imaging measures at the time of acute HSI with longitudinal clinical outcomes, including time to RTS and reinjury.

Methods

The data presented in this study were collected as part of a larger prospective cohort investigation of collegiate athletes who sustained an HSI. The study was approved by the University's Health Sciences Institutional Review Board, and participants provided written informed consent prior to enrollment.

Study Design

Collegiate football, soccer, and track athletes who sustained a unilateral HSI confirmed by a member of the respective teams' sports medicine staff were included in this study. An HSI was diagnosed as sudden onset of posterior thigh pain that occurred during a sport-related activity that resulted in the athlete not being able to return for at least one practice or competition, and the presence of two or more of the following during clinical examination: palpable pain along the hamstring muscles, posterior thigh pain without radicular symptoms during a passive straight leg raise, and/or weakness or pain with resisted knee flexion.[62] Participants were excluded from this analysis if imaging data was not captured within seven days of the HSI or if there was not an imaging confirmed HSI identified by a musculoskeletal radiologist (KL, RK). The presence of injury on T2-weighted MR was identified as a region of architectural disruption of the hamstring muscle complex and/or hyperintense signal within the

hamstrings, most likely representing injury associated edema. Athletes with distinct injuries of each limb that occurred at different timepoints within the study observation window were allowed to be included in the analysis, however when an athlete sustained multiple injuries of the same limb within the observation window, only imaging data from the first HSI was included in the analysis.

A standardized rehabilitation protocol was implemented by the teams' athletic trainer, and RTS was determined when medical clearance was obtained to resume all sport-related activities. RTS clearance was based on a combination of factors including full hamstring range of motion, minimal to no pain with hamstring palpation, and no apprehension with on-field sports-specific movements. Following RTS, all athlete reinjuries were tracked by the team athletic trainers. Reinjuries were defined as an acute HSI to the same limb as the index HSI, requiring the athlete to miss at least one practice or competition within a 12-month period after RTS. Any HSIs involving the contralateral limb, relative to the index HSI, were not included as a reinjury.

Magnetic Resonance Imaging Protocol

Participants received an MRI examination of bilateral upper thighs, completed on a 3.0T scanner (GE HealthCare Discovery MR750, Waukesha, WI) using a 32-channel full torso coil and positioned in a feet-first supine position in the scanner. A 3D axial T1-weighted spoiled gradient recalled echo (SPGR) sequence was used for anatomical reference with the following parameters: no fat saturation, TR/TE = 5.9/2.1 ms, flip = 15 degrees, FOV = 44 cm, matrix = 640x640 (reconstructed at 1024x1024), 80 slices, 5 mm thick, bandwidth = 195 Hz/pixel, PURE intensity correction. A T2-weighted fast recovery fast spin echo (FR-FSE) sequence was used to identify muscle edema in the region of injury with the following parameters: fat/water separation with iterative decomposition of water and fat with echo asymmetry and least-squares

estimation (IDEAL), TR/TE = 4,473/85.0 ms, matrix = 448 x 448 (reconstructed to 512 x 512), 44 slices, 7 mm thick, 2 mm spacing, bandwidth = 140 Hz/pixel. Diffusion-weighted images were acquired in two slabs using spin-echo echo planer imaging (SE-EPI) with weighting in 30 uniformly distributed directions on a unit sphere, 6 non-diffusion-weighted volumes (b=0 images), b-value of 500 s/mm^2, and other parameters: TR/TE = 5770/51.1 ms, FOV = 48 cm, matrix = 160x160, 72 slices, 3 mm thick. The diffusion acquisition was repeated twice with reversed phase-encode directions (anterior-posterior and posterior-anterior) to correct for susceptibility-induced distortions.

Magnetic Resonance Imaging Analysis

Clinical interpretations of the HSI were performed by one of two musculoskeletal radiologists (RK, KL), each with over 20 years of experience. The primary muscle of injury was identified and the location and severity of injury was evaluated using the BAMIC[6] scoring system, which assesses the overall injury grade (0-4) and site classification (myofascial [a], musculotendinous [b], intratendinous [c]), and was assessed using the T1- and T2-weighted sequences.

For diffusion-weighted data, distortion, eddy current, and motion correction were performed using FSL TOPUP[33] and EDDY.[34] [80] Data were filtered using a local principal component analysis filter,[35] then linear fitting to a diffusion tensor (DTI) model was performed with FMRIB Diffusion Toolbox (FDT, FMRIB Software Library, Oxford, UK). When small misalignments between T1- and diffusion-weighted scans occurred, they were manually registered with visual confirmation. Quantitative scalar measures were computed from DTI images, including fractional anisotropy (FA), mean diffusivity (MD), radial diffusivity (RD), and principal effective diffusivity eigenvalues (λ_1, λ_2, λ_3) and were calculated using FMRIB's Diffusion Toolbox (FMRIB Software Library, Oxford, UK).[80]

Anatomical three-dimensional contours of each hamstring muscle (biceps femoris short head, biceps femoris long head, semitendinosus, semimembranosus) of bilateral thighs were completed via manual segmentation using T1-weighted axial SPGR images (FSLeyes, v1.5.0, Oxford, UK).[81] Using the T2-weighted image, musculoskeletal radiologists (KL, RK) identified the region of increased signal that was associated with a HSI. Manual segmentation was used to identify all voxels within this region (**Figure 3.1**) (FSLeyes, v1.5.0, Oxford, UK) [81] and was further refined by taking the intersection of the muscle boundaries and the representative region. The resulting region was used to represent the region of injured muscle tissue. Edema volume within the hamstring muscles was calculated by multiplying voxels identified as containing edema within the muscle boundaries by voxel volume. To account for differences in subject body habitus, volumes were normalized by the height-mass product.[88]

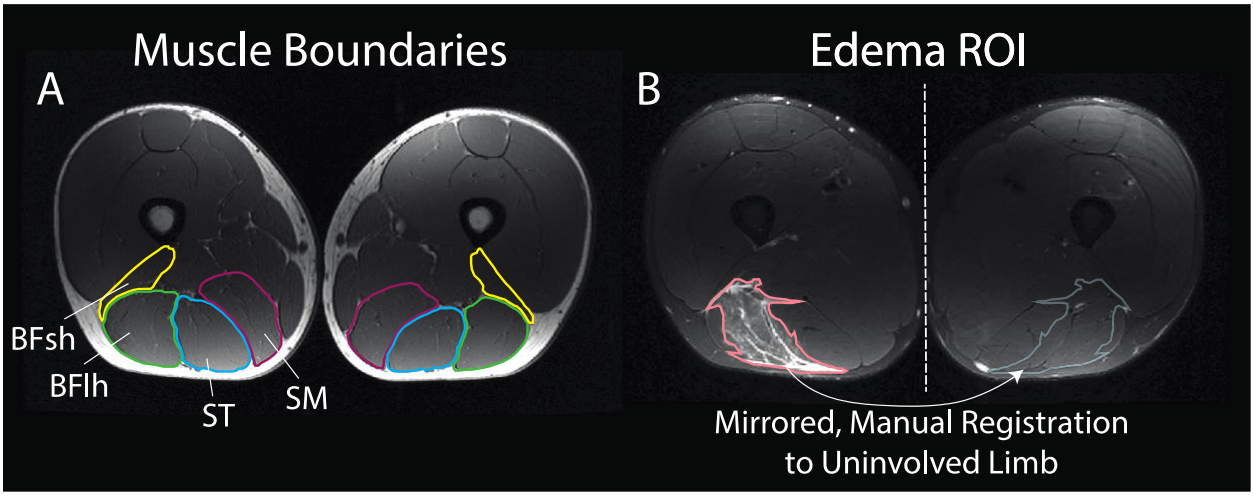

Figure 3.1. Mean quantitative diffusion metrics were calculated within manually outlined regions of interest (ROI) on the injured limb defined by the intersection of **A.)** muscle boundaries and **B.)** edema. For between limb comparisons, ROIs were mirrored and manually registered to the uninvolved limb. Data shown are from one slice of a representative participant.
Biceps femoris short head (BFsh), biceps femoris long head (BFlh), semitendinosus (ST), semimembranosus (SM).

Mask data were down-sampled to match the resolution of diffusion-weighted imaging sequences and the resulting masks were used for the region of injury. Masks representing injury

regions were superimposed over the FA, MD, RD, and principal effective diffusivity eigenvalue (λ_1, λ_2, λ_3) maps to measure the mean values of quantitative DTI outcome measures within the region of injured muscle tissue (MATLAB, v2021b, MathWorks, Natick, MA).

Statistical Analysis

Standard descriptive statistics (means/standard deviations, median/interquartile range, and frequencies/percentages) were used to describe the participants. Imaging outcome measures included: edema volume within the hamstring muscles normalized by height*mass product; BAMIC grade and site classification; and DTI metrics (FA, MD, RD, λ_1, λ_2, λ_3). The associations between imaging outcomes and time to RTS were modeled using a negative binomial regression, and reported as incident risk ratios (IRR) and 95% confidence intervals (CI). The associations between imaging outcomes and reinjury status were determined using generalized estimating equations (GEE) for a binomial outcome with a log link, and reported as odds ratios (OR) and 95% CI. All analyses were conducted using SAS v9.4 (SAS Institutes, Cary, NC) and significance was assessed at $\alpha \leq 0.05$.

Results

Twenty-two unique athletes met eligibility criteria and participated in this study, with four athletes sustaining two distinct injuries, one of each limb, resulting in 26 recorded HSIs (**Figure 3.2**). Participant characteristics at TOI are presented in **Table 3.1**. The median days to RTS was 22 (interquartile range 15-33.5); five reinjuries were recorded (19%) (**Table 3.1**). The biceps femoris long head was the most commonly injured muscle (73%) with BAMIC classification 3c being the most common injury grade and location (31%). Imaging metrics for all HSIs are presented in **Table 3.2**. Representative imaging data for one participant is demonstrated in **Figure 3.3**.

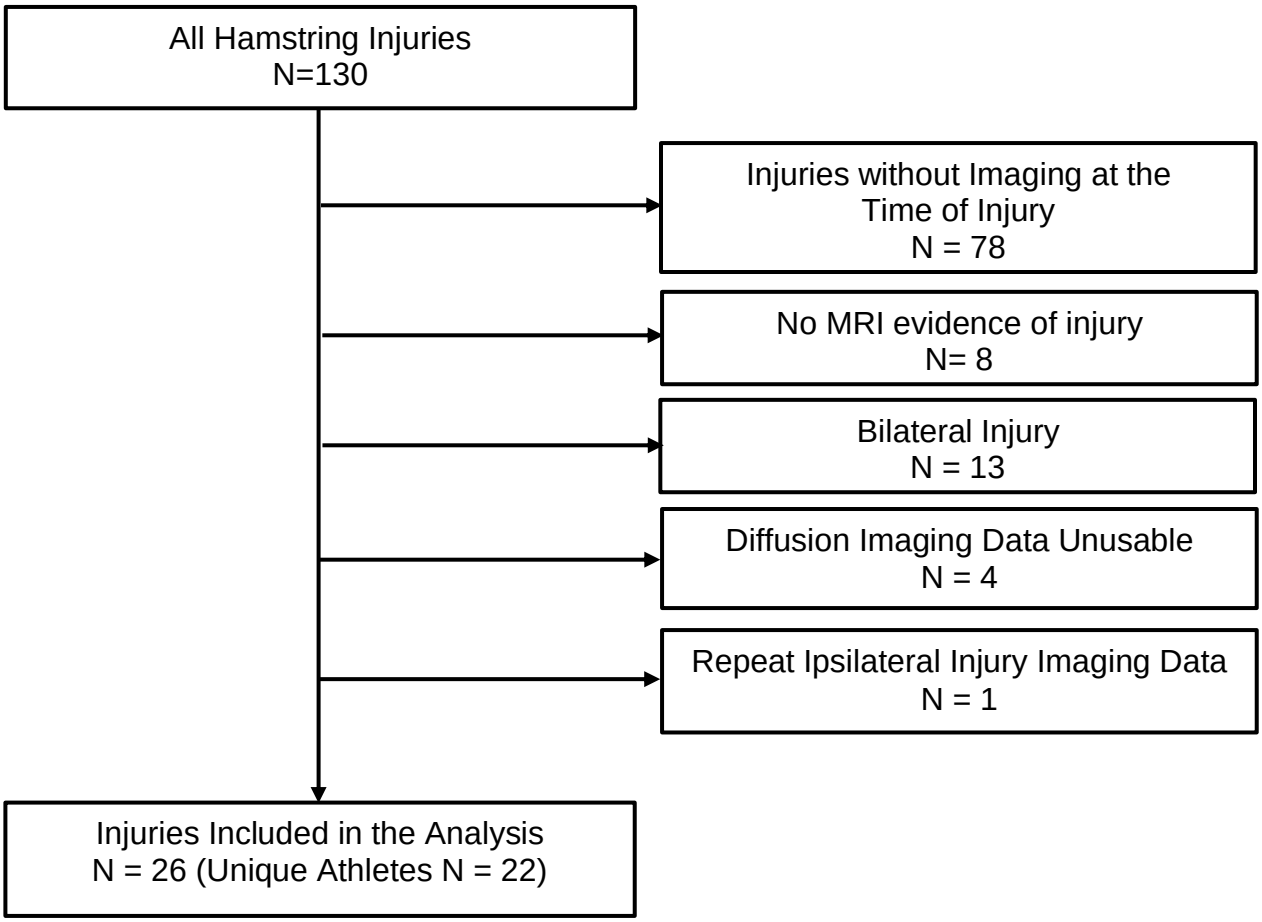

Figure 3.1. Participant inclusion criteria. All participants included in this analysis had unilateral evidence of injury on a T2-weighted magnetic resonance image (MRI) within 7 days of injury. Participants who sustained bilateral injuries linked to the same date/mechanism of injury were excluded from the analysis. If a participant sustained distinct injuries on each limb, both injuries were included in the analysis, however when an athlete sustained repeat ipsilateral injuries within the study observation window, only imaging data from the first injury on that limb was included in the analysis.

Table 3.1. Participant characteristics. Values are reported as counts and means (standard deviations) unless otherwise noted. Percentages are relative to the number of participants within each group summarized in each respective column. For participants with multiple injuries, descriptive statistics are reported for the first injury observed.
IQR = Interquartile Range

		Reinjury	
	All (n = 22)	**Yes (n = 5)**	**No (n = 17)**
Age (years)	19.8 (1.3)	20.2 (1.9)	19.7 (1.9)
Height (m)	1.84 (0.07)	1.86 (0.02)	1.83 (0.02)
Weight (kg)	88.4 (18.4)	87.1 (9.9)	85.4 (9.9)
Sex (% of total participants)			
Male	19 (86%)	5 (100%)	14 (82%)
Female	3 (14%)	0 (0%)	3 (18%)
Sport (% of total participants)			
Football	10 (45%)	1 (20%)	9 (53%)
Track	11 (50%)	4 (80%)	7 (41%)
Soccer	1 (5%)	0 (0%)	1 (6%)
Time to Return to Sport (days) (median, (IQR))	22 (15-33.5)	21 (19-22)	22 (12.5-45)

Table 3.2. Injury characteristics. Values are reported as counts and means (standard deviations) unless otherwise noted. Percentages are relative to the number of injuries recorded in the group summarized in each respective column.

		Reinjury	
	All (n = 26)	**Yes (n = 5)**	**No (n = 21)**
Previous Injury			
Yes	5 (19%)	0 (0%)	5 (24%)
No	21 (81%)	5 (100%)	16 (76%)
Primary Muscle Injured			
Biceps Femoris Short Head	1 (4%)	0 (0%)	1 (5%)
Biceps Femoris Long Head	19 (73%)	4 (80%)	15 (71%)
Semitendinosus	2 (8%)	1 (20%)	1 (5%)
Semimembranosus	4 (15%)	0 (0%)	4 (19%)
British Athletic Muscle Injury Classification			
1a	3 (12%)	2 (40%)	1 (5%)
1b	3 (12%)	0 (0%)	3 (14%)
2a	4 (15%)	0 (0%)	4 (19%)
2b	2 (8%)	2 (40%)	0 (0%)
2c	3 (12%)	1 (20%)	2 (10%)
3a	1 (4%)	0 (0%)	1 (5%)
3b	2 (8%)	0 (0%)	2 (10%)
3c	8 (31%)	0 (0%)	8 (38%)
Muscle Edema ($cm^3/(kg*m)$)	0.46 (0.54)	0.32 (0.15)	0.50 (0.59)
Fractional Anisotropy [-]	0.190(0.024)	0.206 (0.019)	0.187 (0.024)
Mean Diffusivity ($mm^2/s*10^3$)	1.87 (0.15)	1.77 (0.05)	1.90 (0.16)
Radial Diffusivity ($mm^2/s*10^3$)	1.69 (0.15)	1.58 (0.04)	1.71 (0.15)
$\boldsymbol{\lambda_1}$ ($mm^2/s*10^3$)	2.25 (0.17)	2.16 (0.08)	2.27 (0.18)
$\boldsymbol{\lambda_2}$ ($mm^2/s*10^3$)	1.82 (0.15)	1.72 (0.07)	1.85 (0.16)
$\boldsymbol{\lambda_3}$ ($mm^2/s*10^3$)	1.55 (0.14)	1.45 (0.05)	1.58 (0.15)

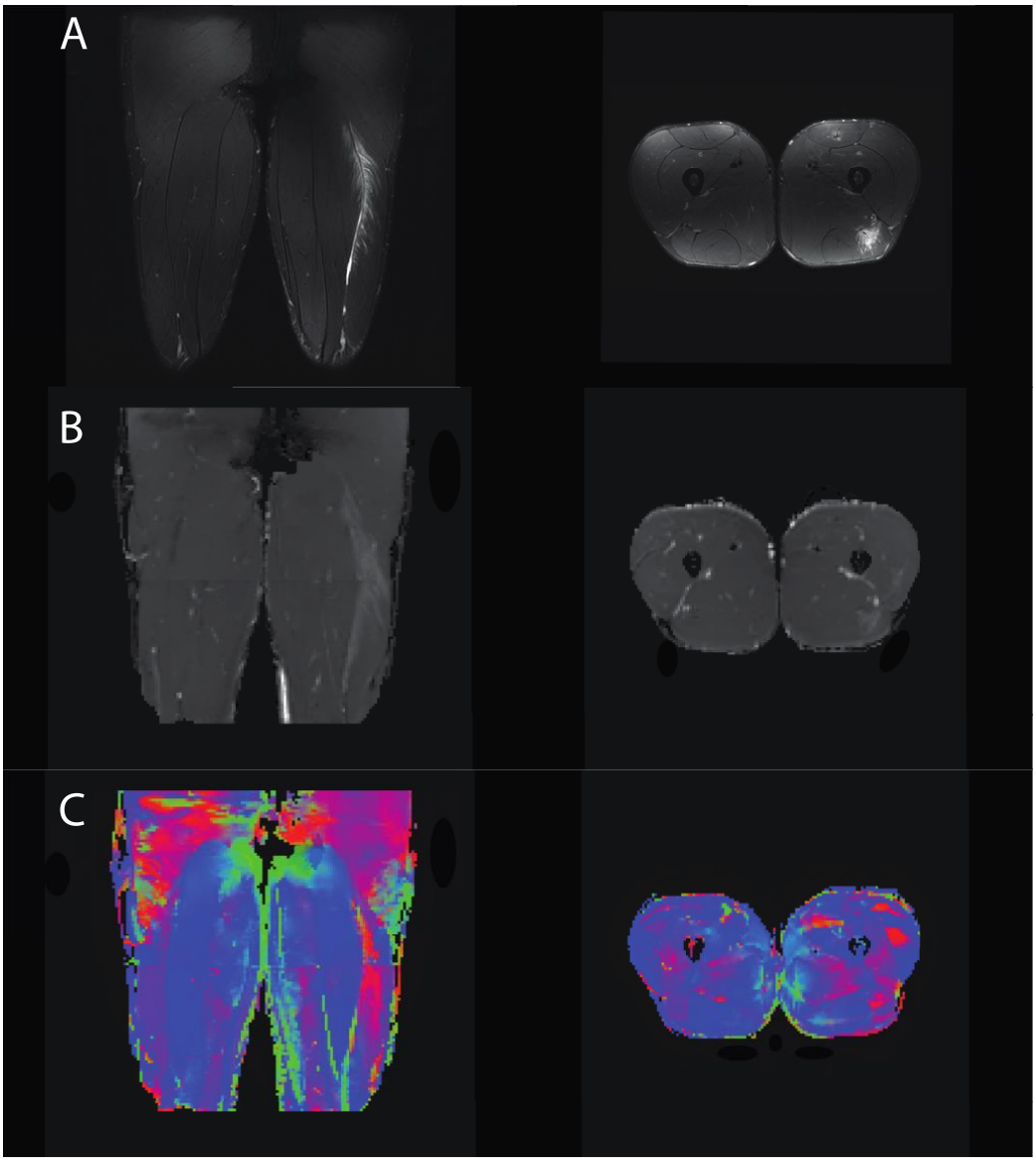

Figure 3.3. Representative imaging data from one participant at time of injury, A.) T2-weighted, B.) mean diffusivity, and C.) primary eigenvalue maps along principal direction (λ_1).

Time to Return to Sport

A significant association was not detected between days to RTS and any imaging measure (normalized muscle edema volume, p = 0.81; BAMIC grade and site, p-values > 0.15; DTI metrics, p-values > 0.11) (**Table 3.3**).

Reinjury

No significant associations were detected between normalized muscle edema volume (p = 0.13), BAMIC injury grade and site (p-values > 0.16), or FA values (p = 0.21) and reinjury. A significant association was detected between all diffusivity metrics except λ_1 and reinjury, with a 1 unit (0.0001 mm/s^2) increase in each of the diffusivity metrics at TOI resulting in the following decreased odds of reinjury: MD (OR: 0.46, 95% CI: 0.24,0.87, p = 0.016), RD (OR: 0.43, 95% CI: 0.23,0.81, p = 0.008), λ_2 (OR: 0.44, 95% CI: 0.24,0.79, p = 0.007), λ_3 (OR: 0.43, 95% CI: 0.23,0.82, p = 0.01). A marginally significant relationship between λ_1 and reinjury was detected (OR: 0.53, 95% CI: 0.27,1.02, p = 0.057) (**Table 3.4**, **Figure 3.4**).

Table 3.3. Negative binomial regression models to determine the association between imaging parameters and return to sport (RTS) days. British Athletic Muscle Injury Classification (BAMIC) system were considered separately as overall as BAMIC grade (0-4) and BAMIC anatomical site (myofascial [a], musculotendinous [b], intratendinous [c]) and included as main effects in the model. Unit represents the unit increase used for interpretation of incident risk ratio (IRR) and 95% confidence interval (CI).
‡Type III p-values based on score test statistic for categorical variable.

Model	Parameter	Unit	IRR	95% CI		p-Value
1	**Muscle Edema** (cm^3/(m*kg))	1	1.04	0.76	1.38	0.81
2	**BAMIC Grade**	1	1.22	0.85	1.75	0.29
	BAMIC Site b (reference a)	1	2.09	1.24	3.53	0.15‡
	BAMIC Site c (reference a)	1	1.48	0.81	2.73	
3	**Fractional Anisotropy** [-]	0.01	1.06	0.99	1.13	0.11
4	**Mean Diffusivity** (mm^2/s)	0.0001	0.92	0.79	1.06	0.25
5	**Radial Diffusivity** (mm^2/s)	0.0001	0.91	0.78	1.05	0.19
6	$\boldsymbol{\lambda_1}$ (mm^2/s)	0.0001	0.94	0.82	1.08	0.40
7	$\boldsymbol{\lambda_2}$ (mm^2/s)	0.0001	0.91	0.78	1.05	0.18
8	$\boldsymbol{\lambda_3}$ (mm^2/s)	0.0001	0.92	0.80	1.05	0.22

Table 3.4. Generalized estimating equation models to determine the relationship of imaging parameters between those that do versus do not go on to reinjure following hamstring strain injury. British Athletic Muscle Injury Classification (BAMIC) system were considered separately as BAMIC grade (0-4) and BAMIC anatomical site (myofascial [a], musculotendinous [b], intratendinous [c]) and included as main effects in the model. Unit represents the unit increase used for interpretation of odds ratio (OR) and 95% confidence interval (CI).
†Model 1 used an independent correlation structure due to the lack of convergence when using an exchangeable correlation structure.
‡Type III p-values based on score test statistic for categorical variable.

Model	Parameter	Unit	OR	95% CI		p-Value
1†	**Muscle Edema** ($cm^3/(m*kg)$)	1	0.43	0.14	1.29	0.13
2	**BAMIC Grade**	1	0.33	0.07	1.55	0.16
	BAMIC Site b (reference a)	1	1.19	0.09	15.80	0.99‡
	BAMIC Site c (reference a)	1	0.95	0.06	14.97	
3	**Fractional Anisotropy** [-]	0.01	1.57	0.78	3.19	0.21
4	**Mean Diffusivity** (mm^2/s)	0.0001	0.46	0.24	0.87	0.016
5	**Radial Diffusivity** (mm^2/s)	0.0001	0.43	0.23	0.81	0.008
6	λ_1 (mm^2/s)	0.0001	0.53	0.27	1.02	0.057
7	λ_2 (mm^2/s)	0.0001	0.44	0.24	0.79	0.007
8	λ_3 (mm^2/s)	0.0001	0.43	0.23	0.82	0.011

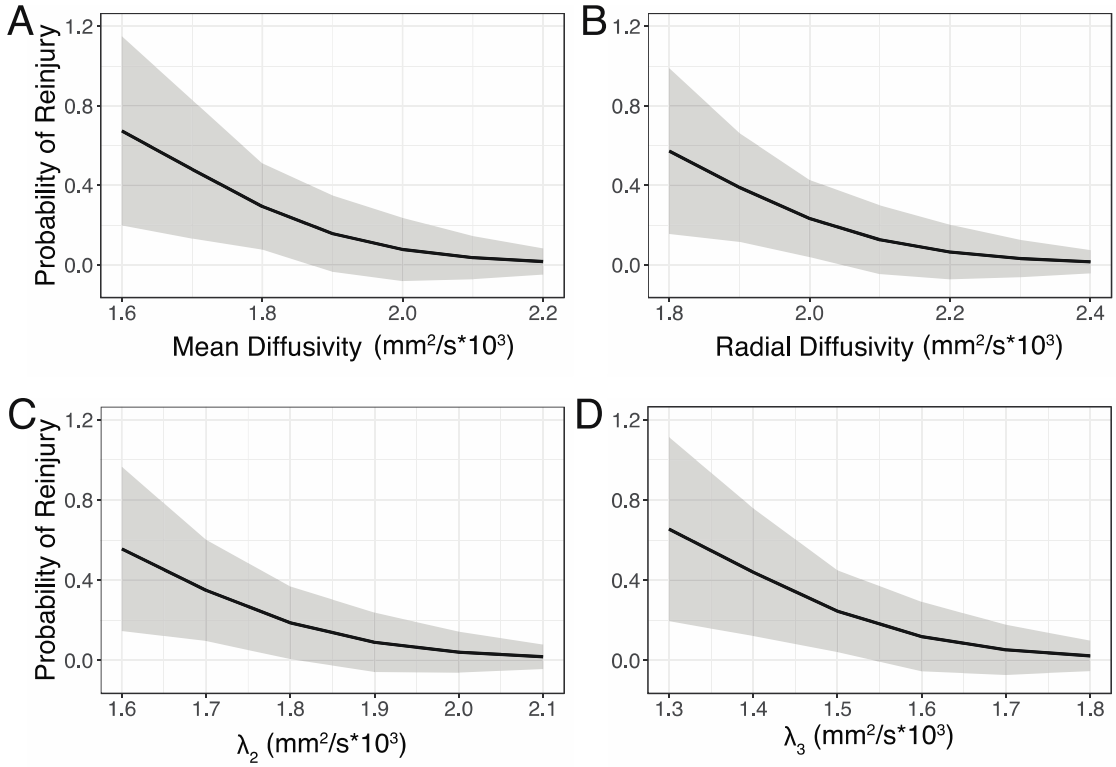

Figure 3.4. Generalized estimating equation model results demonstrating significant relationships with diffusivity metrics **A.)** mean diffusivity, **B.)** radial diffusivity, and principal effective diffusivity eigenvalue **C.)** λ_2 and **D.)** λ_3 in the injured region following acute hamstring strain injury and probability of reinjury.

Discussion

The purpose of this study was to determine the association of MRI-based injury grading and quantitative imaging measures at the time of acute HSI with longitudinal clinical outcomes, including time to RTS and reinjury. While Significant associations were not detected between any imaging measures and days to RTS, greater diffusivity measures (MD, RD, λ_1, λ_2, λ_3) were associated with decreased odds of reinjury.

Time to Return to Sport

We did not detect an association between any of the imaging measures (edema volume, BAMIC injury grading, or quantitative parameters of muscle microstructure) and days to RTS. Although edema volume has been previously investigated, methods used to represent edema volume vary and are often estimated based on a representative slice determined as the greatest extent of injury.[55, 89] To our knowledge, this is the first study that has measured muscle edema volume directly. Despite the elimination of variability in estimated volumes, we still failed to detect an association between edema volume and days to RTS. Because using DTI metrics to represent muscle microstructure is a relatively novel application, only one study to date has investigated DTI metrics and time to RTS following a variety of lower extremity muscle injuries and similarly did not find an association between the two.[10] Despite narrowing the inclusion criteria in the present study to compare across injuries of the hamstrings, we were still unable to detect an association between DTI metrics and time to RTS.

The evidence supporting the association between BAMIC and injury prognosis is mixed. While our findings are consistent with many prior studies that did not find a relationship between BAMIC and days to RTS,[14-16] other studies have demonstrated a significant relationship does exist.[10-13] BAMIC injury classification consists of two components, a grade (0-4) based on the relative amount of hyperintense signal change and a sub-classification based on the anatomical

site (a-c) of injury.[12] Inconsistencies in how each component is used in statistical models to determine clinical associations may contribute to the mixed findings regarding this tool.

Further, differences in study designs and external factors influencing time to RTS may also explain inconsistencies in relationships between TOI imaging measures and clinical outcomes. For example, the inclusion of athletes with and without MRI-confirmed injuries complicates comparisons across studies, as distinct relationships between imaging findings and time to RTS have been identified with athletes that do (MRI-positive) versus do not (MRI-negative) demonstrate injury on imaging.[55, 90, 91] Inclusion of athletes with only MRI-positive injuries in the present study was necessary for the identification of all imaging parameters. However, the more focused inclusion criteria may have contributed to the lack of identified relationships. Finally, ranges of time to RTS often vary greatly within and across studies, potentially due to the differences in study populations and the influence of external factors such as RTS criteria, timing relative to the competitive season, and exposure after RTS. While imaging measures at TOI may still hold relevant relationships with long-term outcomes following HSI, future studies will need a rigorous study design to account for external factors and challenges associated with using time to RTS as an outcome measure. Consideration of interval assessments of recovery independent of time to RTS or other measures of longitudinal outcomes such as resolution of strength or performance may be warranted.

Reinjury

Of the 26 index HSIs, 5 (19%) went on to reinjure within 12 months. Consistent with a recent review,[50] our findings demonstrate that TOI MRI-based injury assessments at the gross anatomical level are not associated with reinjury. Conversely, DTI measures of muscle microstructure indicate that decreased diffusivity measures (MD, RD, λ_1, λ_2, λ_3) were associated with greater odds of reinjury.

In the presence of muscle injury, less restricted diffusion is expected due to compromise of structural integrity of the sarcolemma, which affects the permeability of water exchange between intra- and extracellular compartments. This would be consistent with changes in diffusivity parameters including increased diffusivity in principal eigenvalues (λ_1, λ_2, λ_3), increased MD, RD, and decreased microstructural organization (FA). Preliminary evidence indicates these trends exist following acute muscle strain injuries.[10, 18-20] Given that increased diffusivity measures are consistent with the physiological processes expected with an acute muscle strain injury, it is probable that a more severe injury would be associated with increased measures of diffusivity and decreased values of tissue organization (FA) and thus more likely to reinjure. However, the opposite was true in our study, with those who reinjured demonstrating a decrease in diffusivity measures (MD, RD, λ_1, λ_2, λ_3) compared to those who do not reinjure. Findings from the current study demonstrating that those who go on to reinjure have muscle microstructural metrics more typical of non-injured tissue at the time of the index injury is likely a result of external factors not captured by imaging. Although the relationship of diffusion changes in the presence of injury is complex,[25] it is likely that external factors such the state of muscle microstructure at RTS or the relative amount of recovery compared to TOI may play a role in the directional relationship observed in this study.

Limitations

The validity of DTI metrics used to represent muscle microstructure has been established.[78, 79] However, the clinical utility of these measures has not been extensively studied. Although the focus of the present analysis was to address this research gap by focusing on the independent relationships between quantitative MRI-based characteristics of injury and clinical outcomes, HSIs are known to be multifactorial.[50] The investigation of potential interactions between imaging measures and additional risk factors such as prior injury

and exposure after RTS is warranted. Although the sample size of injuries and reinjury rate observed in the present study is consistent with prior prospective studies,[10, 13] accounting for an extensive list of potential contributing factors to explain clinical outcomes following HSI will require a larger sample with adequate power. Furthermore, although the study design of the present study was prospective, the high variability in days to RTS and the low number of reinjuries limits the predictive ability of the relationships identified. The challenges and increased complications associated with HSIs continue to support the investigation of prognostic indicators to improve injury management. Future investigations may consider relative changes in quantitative imaging measures throughout recovery and at the time of RTS to fully define the utility of MRI following HSI.

Conclusions

MRI-based measures of injury classification (BAMIC) and muscle edema volume assessed at time of hamstring strain injury were not associated with days to RTS or reinjury. Similarly, a significant association between quantitative diffusion parameters at TOI and days to RTS was not detected. However, those who went on to reinjure demonstrated decreased quantitative diffusion parameters within the injured muscle at TOI compared to those who do not reinjure. Despite recent advancements in the ability of MRI to measure muscle microstructure through DTI, the relationship between TOI imaging assessment and longitudinal clinical outcomes remains complicated. Additional work is warranted to further understand the relationship between DTI metrics and reinjury status and the influence of external factors on the relationship between TOI imaging measures and longitudinal clinical outcomes.

Chapter 4.

Association of quantitative imaging measures at the time of return to sport following acute hamstring strain injury with eccentric hamstring strength and reinjury incidence

Christa M. Wille, Samuel A. Hurley, Mikel R. Stiffler-Joachim, Kenneth Lee, Richard Kijowski, Bryan C. Heiderscheit

Abstract

Hamstring strain injuries (HSI) are a common occurrence in athletics and complicated by high rates of reinjury. Evidence of remaining injury observed on magnetic resonance imaging (MRI) at the time of return to sport (RTS) may be associated with strength deficits and prognostic for reinjury, however, conventional imaging has failed to establish a relationship. Quantitative measure of muscle microstructure using diffusion tensor imaging (DTI) may hold potential for assessing a possible association between injury-related structural changes and clinical outcomes. The purpose of this study was to determine the association of RTS MRI-based quantitative measures, such as edema volume, muscle volume, and DTI metrics, with clinical outcomes (i.e., strength and reinjury) following HSI. Spearman's correlations and Firth logistic regressions were used to determine relationships in between-limb imaging measures and between-limb eccentric strength and reinjury status, respectively. Twenty injuries were observed, with four recorded reinjuries. Eccentric hamstring strength had a significant association with principal effective diffusivity eigenvalue λ_1 ($r = -0.64$, $p = 0.003$) and a marginal association with mean diffusivity ($r = -0.46$, $p = 0.056$). Significant relationships between other MRI-based measures of morphology and eccentric strength were not detected, as well as between any MRI-based measure and reinjury status. In conclusion, DTI may track changes in hamstring muscle microstructure that relate to eccentric strength that are not captured by conventional imaging at the whole muscle level.

Introduction

Hamstring strain injuries (HSI) are common in athletics and result in significant loss of time from activity, decreased quality of life,[48] and increased financial burden in elite sports.[49] High reinjury rates further complicate the management of HSI[51, 52] with strength and morphological deficits known to persist following injury. At the time of RTS, the injured limb shows strength deficits compared to the contralateral limb, as well as compared to uninjured athletes.[63-66] Changes to the hamstring muscle-tendon structure such as reduced biceps femoris fascicle length[41] and biceps femoris atrophy,[65] are known to persist following HSI and may contribute to this reduced strength following HSI.

Hamstring strength deficits at the time of RTS are thought to be linked to evidence of remaining injury observed on magnetic resonance imaging (MRI).[65] While most studies[56, 65, 70, 71] quantify remaining injury based on MRI measures from fluid-sensitive sequences observed at the gross-anatomical level (e.g. length, cross sectional area, volume of hyperintensity), more recent studies explored qualitative changes at the tissue level, such as the absence or presence of tendon waviness or discontinuity,[72, 73] muscle fiber tears, or loss of muscle pennation angle.[72] Regardless of the approach used, no clear relationship with HSI reinjury was found.[50]

Recent advancements in musculoskeletal MRI, such as diffusion tensor imaging (DTI), have allowed for a quantitative assessment of muscle microstructure and may hold potential in explaining the relationship between structural and functional deficits known to exist following HSI. DTI generates contrast from the random diffusion of water molecules and utilizes diffusivity differences to infer information about muscle microstructure. While the microstructure of an intact muscle fiber will encourage water to preferentially diffuse along the direction of the fiber, more random diffusion will occur in an injured muscle fiber.[22] Initial work indicates that DTI is sensitive to detect differences in the injured limb following acute HSI and demonstrates resolution of microstructural differences throughout recovery.[18] Further, DTI has been used to

demonstrate an increase in fascicle length following a targeted hamstring strengthening program in a healthy population.[77] However, the associations between DTI parameters at the time of RTS and clinical outcomes, such as hamstring strength and reinjury occurrence, have not yet been explored. Therefore, the purpose of this study was to determine the association of quantitative MRI measures at the time of RTS following HSI with eccentric hamstring strength and reinjury.

Methods

The data presented in this study were collected as part of a larger prospective cohort investigation of collegiate athletes who sustained an HSI. The study was approved by the University's Health Sciences Institutional Review Board, and participants provided written informed consent prior to enrollment.

Study Design

Collegiate football, soccer, and track athletes who sustained a unilateral HSI confirmed by a member of the respective teams' sports medicine staff were included in this study. An HSI was diagnosed as sudden onset of posterior thigh pain that occurred during a sport-related activity that resulted in the athlete not being able to return for at least one practice or competition, and the presence of two or more of the following during clinical examination: palpable pain along the hamstring muscles, posterior thigh pain without radicular symptoms during a passive straight leg raise, and/or weakness or pain with resisted knee flexion.[62] A standardized rehabilitation protocol was implemented by the teams' athletic trainer, and RTS was determined when medical clearance was obtained to resume all sport-related activities. RTS clearance was based on a combination of factors including full hamstring range of motion, minimal to no pain with hamstring palpation, and no apprehension with on-field sports-specific movements. While imaging data was acquired at both TOI and RTS timepoints, TOI imaging

was used to identify the injury while quantitative imaging-based measures at RTS were used to determine associations with clinical outcomes. Participants were excluded from this analysis if imaging data was not captured within seven days of TOI or RTS or if there was not an imaging-confirmed HSI identified by a musculoskeletal radiologist (KL, RK). The presence of injury on T2-weighted MR was identified as a region of architectural disruption of the hamstring muscle complex and/or hyperintense signal within the hamstrings, most likely representing injury-associated edema. If an athlete sustained multiple injuries during the study observation window, only imaging data from the first HSI was included in the analysis.

Following RTS, all athlete reinjuries were tracked by the team athletic trainers. Reinjuries were defined as an acute HSI to the same limb as the index HSI, requiring the athlete to miss at least one practice or competition within a 12-month period after RTS. Any subsequent HSIs involving the contralateral limb, relative to the index HSI, were not included as a reinjury.

Magnetic Resonance Imaging Protocol

Participants received an MRI examination of bilateral upper thighs, completed on a 3.0T scanner (GE HealthCare Discovery MR750, Waukesha, WI) using a 32-channel full torso coil and positioned in a feet-first supine position in the scanner. A 3D axial T1-weighted spoiled gradient recalled echo (SPGR) sequence was used for anatomical reference with the following parameters: no fat saturation, TR/TE = 5.9/2.1 ms, flip = 15 degrees, FOV = 44 cm, matrix = 640x640 (reconstructed at 1024x1024), 80 slices, 5 mm thick, bandwidth = 195 Hz/pixel, PURE intensity correction. A T2-weighted fast relaxation fast spin echo (FR-FSE) sequence was used to identify muscle edema in the region of injury with the following parameters: fat/water separation with iterative decomposition of water and fat with echo asymmetry and least-squares estimation (IDEAL), TR/TE = 4,473/85.0 ms, matrix = 448 x 448 (reconstructed to 512 x 512), 44 slices, 7 mm thick, 2 mm spacing, bandwidth = 140 Hz/pixel. Diffusion-weighted images were acquired in

two slabs using spin-echo echo planer imaging (SE-EPI) with weighting in 30 uniformly distributed directions on a unit sphere, 6 non-diffusion-weighted volumes (b=0 images), b-value of 500 s/mm^2, and other parameters: TR/TE = 5770/51.1 ms, FOV = 48 cm, matrix = 160x160, 72 slices, 3 mm thick. The diffusion acquisition was repeated twice with reversed phase-encode directions (anterior-posterior and posterior-anterior) to correct for susceptibility-induced distortions.

Magnetic Resonance Imaging Analysis

For diffusion-weighted data, distortion, eddy current, and motion correction were performed using FSL TOPUP[33] and EDDY.[34, 80] Data were filtered using a local principal component analysis filter,[35] then linear fitting to a diffusion tensor (DTI) model was performed with FMRIB Diffusion Toolbox (FDT, FMRIB Software Library, Oxford, UK). When small misalignments between T1- and diffusion-weighted scans occurred, they were manually registered with visual confirmation. Quantitative scalar measures analyzed from DTI images included the principal effective diffusivity eigenvalues (λ_1, λ_2, λ_3), fractional anisotropy (FA), mean diffusivity (MD), and radial diffusivity (RD) and were calculated using FMRIB's Diffusion Toolbox (FMRIB Software Library, Oxford, UK).[80]

Anatomical three-dimensional contours of each hamstring muscle (biceps femoris short head (BFsh), biceps femoris long head (BFlh), semitendinosus (ST), semimembranosus (SM)) of bilateral thighs were completed via manual segmentation using T1-weighted axial SPGR images (FSLeyes, v1.5.0, Oxford, UK).[81] Hamstring muscle volume was calculated by multiplying voxels identified within the muscle boundaries by voxel volume. Total hamstring volume was identified by summing the volume across all hamstring muscles (BFsh, BFlh, ST, SM). In descriptive reports of muscle volume, data were normalized by the individual's height-mass product to account for differences in subject body habitus.[88]

Using the T2-weighted image at TOI, musculoskeletal radiologists (KL, RK), each with over 20 years of experience, identified the region of increased signal that was associated with a HSI and identified the primary muscle of injury. Manual segmentation was used to identify all voxels within this injured region (FSLeyes, v1.5.0, Oxford, UK)[81] and was further refined by taking the intersection of the muscle boundaries and the representative region. Injury ROIs from TOI were registered to imaging data collected at RTS using a 12 degree-of-freedom affine registration[82] performed on each limb individually (FSL, FMRIB Software Library, Oxford, UK). The estimated transform was applied to the injury ROI and manually adjusted as needed (**Figure 4.1**).

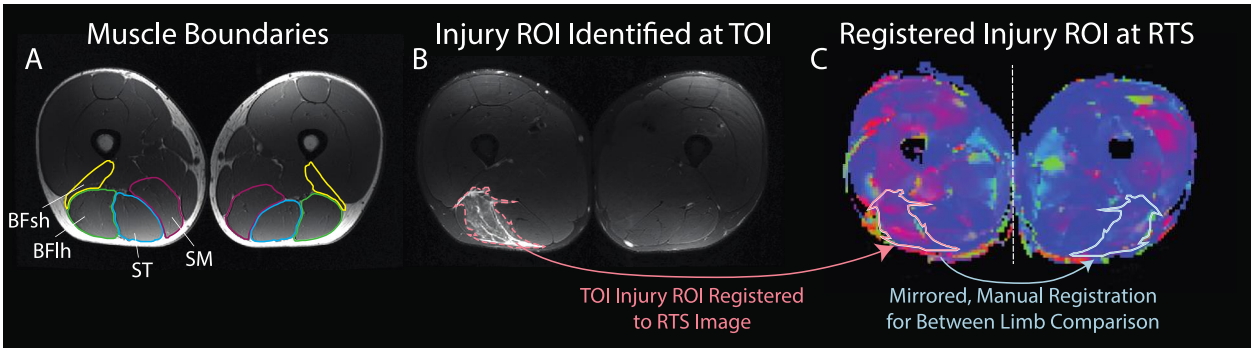

Figure 4.1. Mean quantitative diffusion metrics were calculated within manually outlined regions of injury (ROI) on the injured limb defined by the hyperintense region of signal on T2-weighted imaging at the time of injury (TOI). Injury ROIs were registered to follow up scans at return to sport (RTS) (peach arrow). For between limb comparisons, ROIs were mirrored and manually registered to the uninvolved limb (white arrow). Data shown are from one slice of a representative participant. Biceps femoris short head (BFsh), biceps femoris long head (BFlh), semitendinosus (ST), semimembranosus (SM).

Using the T2-weighted image at RTS, experienced musculoskeletal radiologists (KL, RK) again identified the region of increased signal associated with HSI, and manual segmentation of all voxels within the injured region was completed. Edema volume at RTS within the hamstring muscles was calculated by multiplying voxels identified as containing edema within the muscle boundaries by voxel volume. Edema volumes were normalized by the height-mass product.[88]

Injury ROI masks were down-sampled to match the resolution of diffusion-weighted imaging sequences and superimposed over the FA, MD, RD, and principal effective diffusivity

eigenvalue (λ_1, λ_2, λ_3) maps to measure the mean values of quantitative DTI outcome measures within the identified injured region (MATLAB, v2021b, Mathworks, Natick, MA). Injury ROI masks were also used to generate three-dimensional triangulated surface meshes of the muscle boundaries using the MATLAB-based iso2mesh toolbox.[92]

DTI tractography was performed to determine fascicle length using a deterministic fiber tracking algorithm.[93] Fiber tracts were propagated bi-directionally from seed points placed on a 3 x 3 x 3 mm grid within each muscle. The endpoints of fiber tracts were defined by the borders of segmentation or by stopping criteria defined as follows: $0.1 \leq FA \leq 0.5$, step size = 1.5 mm, and maximum turning angle = 15°.[36] Only fiber tracts that had lengths larger than 20 mm and smaller than 200 mm were included.[30] Fiber tracts were then fit with a three-dimensional 3rd order polynomial curve. The slopes at both endpoints of the curve were calculated, and the endpoints were extended by linearly projecting the slopes on to the muscle surface. The polynomial curve including the extensions is referred to as a muscle fascicle. Fascicle length was calculated as the length of the polynomial curve including the extensions. Only fascicles whose extensions were less than 30% of the total fascicle length were included in further analyses.[30] Due to the known differences that exist in fascicle lengths across the hamstring muscles,[94] only fascicles of the primary injured muscle that passed through the injured region within that muscle were considered for analysis (**Figure 4.2**). Median fascicle lengths were analyzed for each subject to account for non-normal distribution and outliers within each muscle. Participants who had distinct, non-anatomically plausible irregularities in tractography data due to the stitching across slabs were excluded in analyses involving fascicle length.

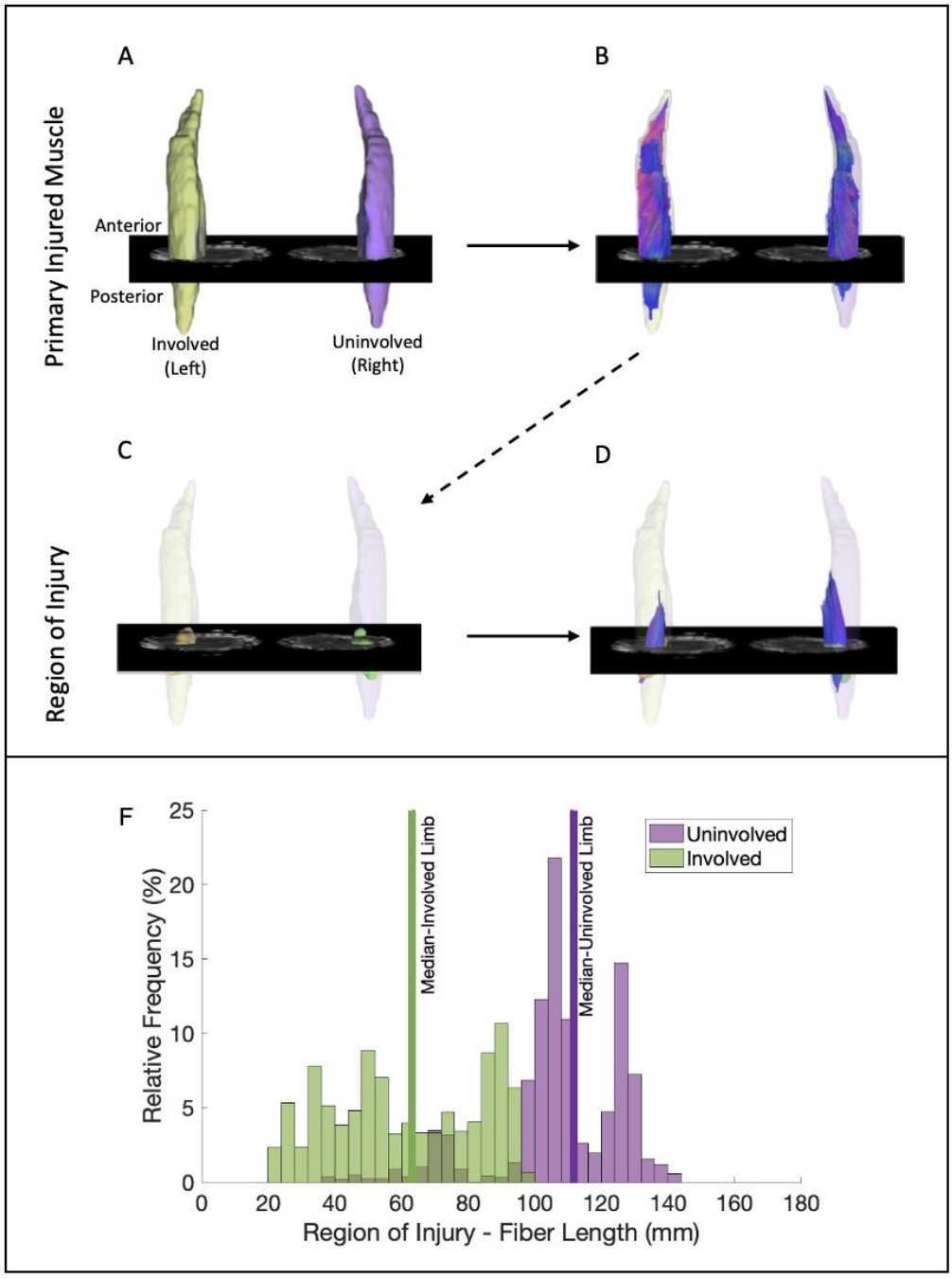

Figure 4.2. Representative imaging data from one participant demonstrating the process used to identify fascicles passing through the region of injury. **A.** Three-dimensional surface mesh generated from manual muscle boundary segmentation of the primary injured muscle (biceps femoris long head); **B.** Identification of all fascicles within the muscle boundary of interest; **C.** Three-dimensional surface mesh generated from manual segmentation of voxels containing increased signal intensity on the T2-weighted fluid sensitive sequence used to represent the region of injury and the mirrored, manually registered region on the uninvolved limb; **D**. Identification of fascicles within the primary injured muscle that pass through the region of injury on the involved limb relative to the uninvolved limb; **E.** Histogram of the relative frequency and median length of fascicles within the primary injured muscle on the involved limb (green) relative to the uninvolved limb (purple).

Eccentric Strength Measurement

Eccentric hamstring strength was measured using the NordBord Hamstring Testing System (Vald Performance, Newstead, QLD, Australia) in accordance with a previously described protocol.[95] The athlete kneeled on a padded platform with each ankle secured in a hook immediately superior to the lateral malleoli. Each hook was in line with a load cell for force measurement. Athletes were instructed to slowly lower themselves, resisting with their hamstrings, with arms across the chest and with shoulders, knees, and hips kept in a straight line. Three warm-up trials were performed, one each at 50%, 75%, and 90% of maximal effort. Following warm-up trials, athletes completed three trials at maximal effort with bodyweight resistance only. Athletes were given a 30-s rest after the warm-up trials and each maximum effort trial. Verbal encouragement was given throughout the trials to incite maximal effort. Trials were accepted if the athlete maintained proper alignment during the trial, a distinct peak in maximal force output followed by a rapid decline was observed, and peaks were within 20% across the three trials. Up to two additional trials were performed if a distinct peak was not reached or the maximum force was more than 20% different from previous trials. Data from all trials were recorded, with the maximum force obtained for each limb out of all trials utilized for analysis.

Statistical Analysis

Standard descriptive statistics (means/standard deviations, median/interquartile range, and frequencies/percentages) were used to describe the participants. Imaging outcome measures included: edema volume within the hamstring muscles normalized by height*mass product, total hamstring muscle volume, primary muscle volume, DTI metrics (FA, MD, RD, λ_1, λ_2, λ_3), and DTI tractography derived muscle fascicle length. Clinical outcomes included

eccentric strength at time of RTS and reinjury incidence. In order to control for between-subject differences, all eccentric strength values and all imaging measures, except edema volume, were reported as between-limb percent differences ([Uninvolved-Involved]/Uninvolved*100). Given exclusion criteria eliminated bilateral injuries in this analysis, edema volume was relative to the involved limb only and thus reported as a continuous, numerical measure. The associations of edema volume and between-limb percent differences in imaging outcomes and between-limb percent differences eccentric strength were modeled using a Spearman's Correlation. The associations of edema volume and between-limb percent differences in imaging outcomes and reinjury status were determined using a firth logistic regression for a binomial outcome, and reported as odds ratios (OR) and 95% confidence intervals (CI). All analyses were conducted using SAS v9.4 (SAS Institutes, Cary, NC) and significance was assessed at $\alpha \leq 0.05$.

Results

Twenty unique athletes met eligibility criteria and were included in this study (**Figure 4.3**). Participant characteristics are presented in **Table 4.1**. The median days to RTS was 22 (interquartile range 21-37; four reinjuries were recorded (20%) (**Table 4.1**). The biceps femoris long head was the most commonly injured muscle (87.5%). Between-limb differences for eccentric hamstring strength and all imaging metrics at the time of RTS are presented in **Table 4.2**. Representative imaging data for one participant are shown in **Figure 4.4**. Fascicle length data were excluded for one participant due to distinct, non-anatomically plausible irregularities associated with stitching raw diffusion data across slabs.

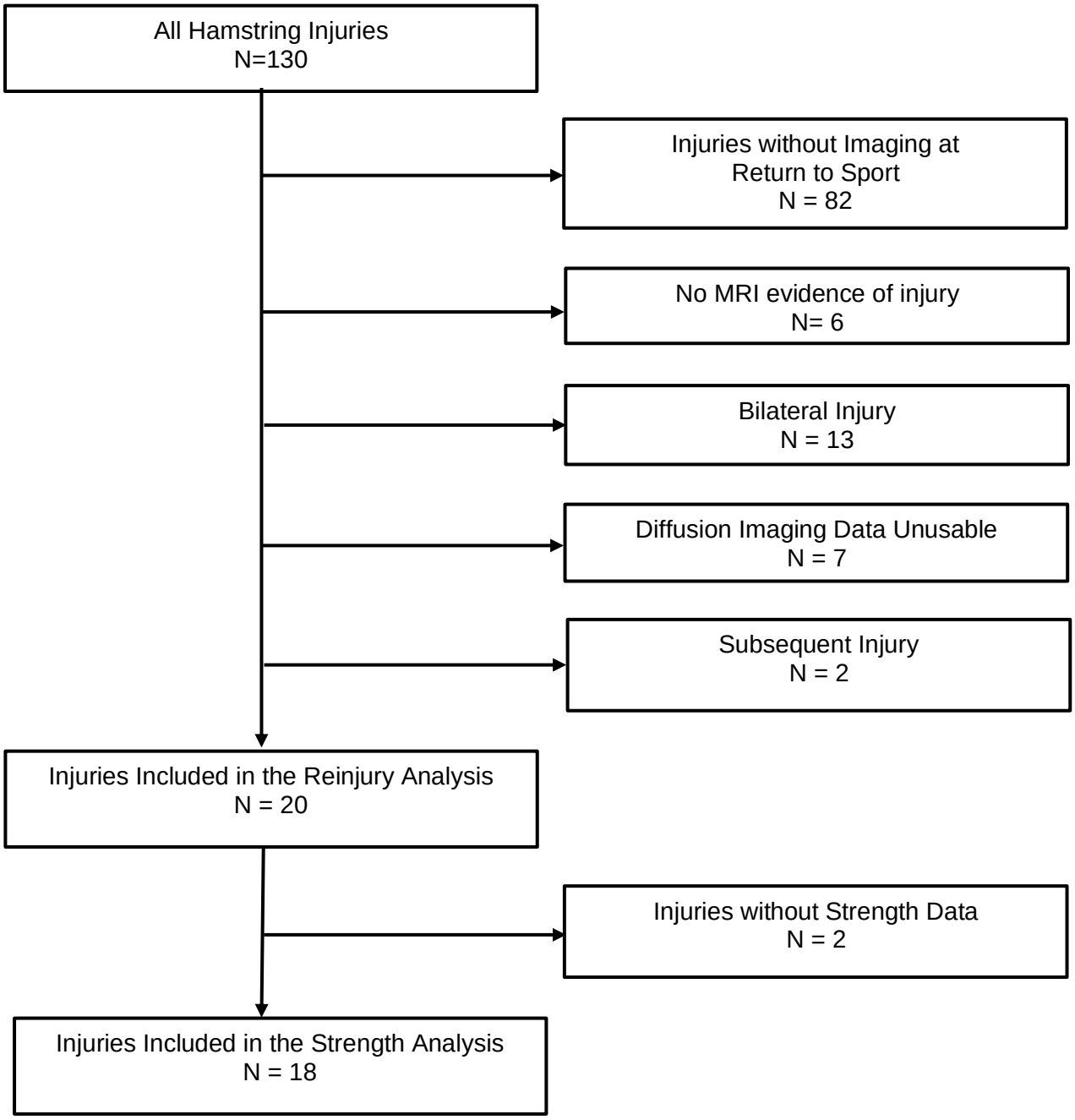

Figure 4.3. Participant inclusion criteria. All participants included in this analysis had unilateral evidence of injury on a T2-weighted magnetic resonance image (MRI) within 7 days of injury. Participants who sustained bilateral injuries linked to the same date/mechanism of injury were excluded from the analysis.

Table 4.1. Participant characteristics. Values are reported as counts (% of total participants) and means (standard deviations) unless otherwise noted. Percentages are relative to the number of participants within each group summarized in each respective column. For participants with multiple injuries, descriptive statistics are reported for the first injury observed. IQR = Interquartile Range

		Reinjury	
	All (n = 20)	**Yes (n = 4)**	**No (n = 16)**
Age (years)	19.7 (1.3)	20.5 (1.9)	19.5 (1.0)
Height (m)	1.83 (0.08)	1.86 (0.03)	1.82 (0.08)
Weight (kg)	86.5 (21.4)	83.2 (5.7)	87.3 (23.9)
Sex			
Male	16 (80%)	4 (100%)	12 (75%)
Female	4 (20%)	0 (0%)	4 (25%)
Sport			
Football	9 (45%)	1 (25%)	8 (50%)
Track	9 (45%)	3 (75%)	6(37.5%)
Soccer	2 (10%)	0 (0%)	2 (12.5%)
Time to Return to Sport (days) (median, (IQR))	22 (21-36.75)	22 (22-22.5)	22 (18-49)
Previous Involved Limb Injury			
Yes	3 (15%)	1 (25%)	2 (12.5%)
No	17 (85%)	3 (75%)	14 (87.5%)
Primary Muscle Injured			
Biceps Femoris Short Head	0 (0%)	0 (0%)	0 (0%)
Biceps Femoris Long Head	17 (85%)	3 (75%)	14 (87.5%)
Semitendinosus	2 (10%)	1 (25%)	1 (6.25%)
Semimembranosus	1 (5%)	0 (0%)	1 (6.25%)

Table 4.2. Eccentric hamstring strength and imaging metrics from the region of injury reported per limb and as a measure of between limb percent difference ([uninvolved-involved]/uninvolved*100). Values are reported as means (standard deviation).

	Involved Limb	**Uninvolved Limb**	**Percent Difference (%)**
Eccentric Hamstring Strength (N/kg)	4.33 (1.02)	4.46 (0.95)	2.8 (9.2)
Muscle Edema ($cm^3/(m*kg)$)	0.122 (0.144)	-	-
Total Hamstring Volume ($cm^3/(m*kg)$)	7.29 (1.10)	7.21 (0.99)	-1.06 (5.0)
Primary Muscle Volume ($cm^3/(m*kg)$)	2.01 (0.42)	1.95 (0.34)	-2.66 (7.13)
Fascicle Length (mm)	67.9 (27.0)	79.6 (27.8)	11.9 (24.2)
Fractional Anisotropy [-]	0.200 (0.024)	0.195 (0.025)	-3.91 (14.5)
Mean Diffusivity (mm^2/s)	1.75 (0.06)	1.69 (0.07)	-3.57 (4.34)
Radial Diffusivity (mm^2/s)	1.56(0.05)	1.51 (0.06)	-3.53 (5.43)
$\boldsymbol{\lambda_1}$ (mm^2/s)	2.13 (0.10)	2.06 (0.01)	-3.69 (4.01)
$\boldsymbol{\lambda_2}$ (mm^2/s)	1.69 (0.07)	1.61 (0.07)	-4.62 (6.03)
$\boldsymbol{\lambda_3}$ (mm^2/s)	1.44 (0.05)	1.41 (0.06)	-2.32 (5.54)

Figure 4.4. Representative imaging data from one participant at return to sport, **A**.) T2-weighted, **B**.) mean diffusivity, and **C**.) primary eigenvalue maps along principal direction.

Between-limb Strength at Return to Sport

A significant association was detected between eccentric hamstring strength and λ_1 (r = *-0.64, p* = 0.003), while a marginal association was observed with MD (r = *-0.46, p* = 0.056) **(Table 4.3, Figure 4.5)**. Significant associations were not detected between eccentric strength and normalized muscle edema volume, total hamstring muscle volume, primary injured muscle volume, fascicle length, FA, RD, λ_2, or λ_3 (p-values $\geq$ 0.10).

Table 4.3. Spearman correlation coefficients *r* for eccentric hamstring strength versus quantitative imaging measures. All variables, except muscle edema volume (involved limb only), were compared as a between limb percent difference.

	Spearman Correlation Coefficients *r*	95% CI		p-Value
Muscle Edema Volume ($cm^3/(m*kg)$)	-0.08	-0.53	0.40	0.76
Total Hamstring Volume	-0.06	-0.51	0.42	0.81
Primary Muscle Injured Volume	-0.23	-0.63	0.27	0.37
Fascicle Length	0.38	-0.13	0.73	0.14
Fractional Anisotropy	-0.33	-0.69	0.16	0.18
Mean Diffusivity	-0.46	-0.76	0.01	0.056
Radial Diffusivity	-0.29	-0.66	0.21	0.25
λ_1	-0.64	-0.85	-0.25	0.003
λ_2	-0.40	-0.73	0.08	0.10
λ_3	-0.18	-0.60	0.31	0.48

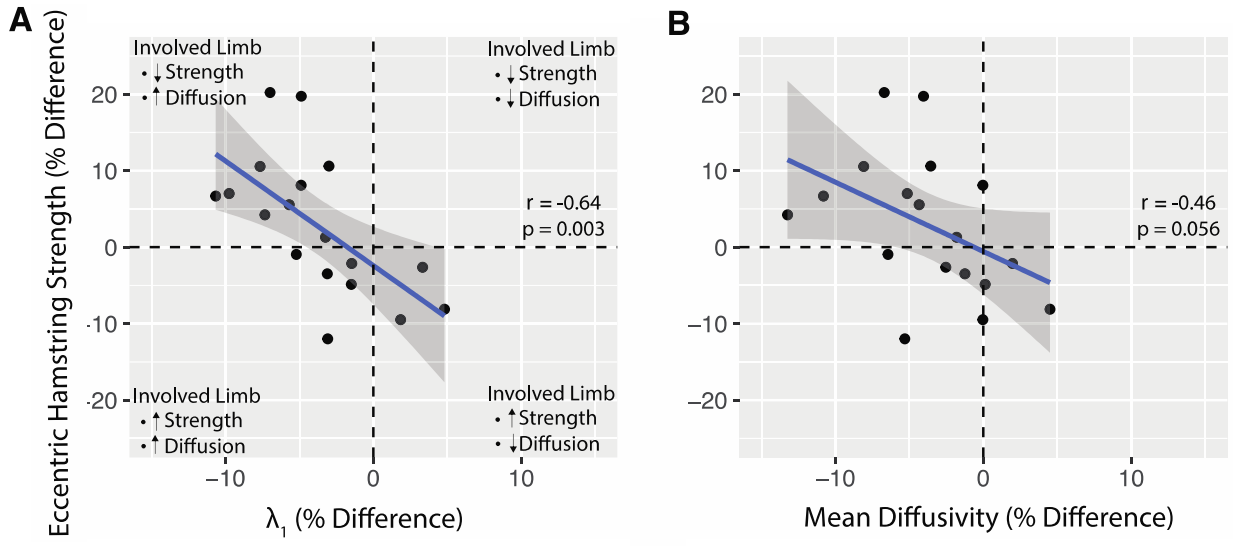

Figure 4.5. Correlations in between-limb eccentric strength and between-limb diffusivity measures: **A**. Principal effective diffusivity eigenvalue λ_1 and **B**. Mean diffusivity.

Reinjury

No significant associations were detected between reinjury and any imaging measure (normalized muscle edema volume, total hamstring muscle volume, primary injured muscle volume, fascicle length, FA, MD, RD, $\lambda 1$, $\lambda 2$, $\lambda 3$; *p*-values ≥ 0.14) **(Table 4.4)**.

Table 4.4. Firth logistic regression models used to determine the relationship of imaging parameters and reinjury incidence following hamstring strain injury. All parameters are reported as a between limb percent difference unless otherwise noted.
OR = Odds Ratio, CI = Confidence Interval.

Parameter	Unit	OR	95% CI		p-Value
Muscle Edema ($cm^3/(m*kg)$)	0.01	0.99	0.87	1.05	0.72
Total Hamstring Volume	1	0.82	0.59	1.03	0.15
Primary Muscle Volume	1	0.96	0.81	1.11	0.62
Fascicle Length	1	0.96	0.90	1.00	0.14
Fractional Anisotropy	1	0.97	0.89	1.04	0.48
Mean Diffusivity	1	0.96	0.76	1.23	0.77
Radial Diffusivity	1	0.99	0.83	1.22	0.95
$\boldsymbol{\lambda_1}$	1	0.91	0.66	1.18	0.52
$\boldsymbol{\lambda_2}$	1	0.99	0.83	1.19	0.89
$\boldsymbol{\lambda_3}$	1	1.00	0.84	1.24	0.99

Discussion

The purpose of this study was to determine the association of quantitative MRI measures at the time of RTS following HSI with eccentric hamstring strength and reinjury. Negative associations were detected when comparing between-limb differences in eccentric hamstring strength and the principal effective diffusivity eigenvalue along the primary direction (λ_1) and MD. That is, athletes who demonstrated decreased strength on the involved limb (more positive % difference) also demonstrated larger diffusivity values (λ_1, MD) on the involved limb (more negative % difference). Significant associations were not detected between any imaging measures and reinjury.

Between-limb Eccentric Strength at Return to Sport

Relationships between muscle DTI metrics and strength measurements have been previously reported in the calf[75, 96] and the back;[74] however, to our knowledge, this relationship has not been explored in an injured population. Despite full medical-clearance for RTS, eccentric strength and microstructural deficits persisted between-limbs for the athletes

included in this analysis. As expected, the majority of athletes who demonstrated a deficit in eccentric hamstring strength on the involved limb (more positive % difference) also demonstrated a corresponding increase in diffusivity metrics (λ_1, MD) in the region of injury on the involved limb (more negative % difference) compared to the uninvolved limb. In the presence of muscle injury, less restricted diffusion is expected due to compromise of structural integrity of the sarcolemma, which affects the permeability of water exchange between intra- and extracellular compartments.[25] This would be consistent with changes in diffusivity parameters including increased diffusivity in principal eigenvalues (λ_1, λ_2, λ_3), increased MD and RD, and decreased microstructural organization (FA). Thus, the greater diffusivity values observed in the involved limb relative to the uninvolved limb at the time of RTS suggests the presence of residual injury.

A significant association between eccentric strength and diffusivity measures λ_2, λ_3, RD, or FA as a representative measure of tissue organization was not detected in this study. Similarly, a recent study characterizing DTI changes in hamstring muscle after HSI did not detect a between-limb difference in FA measures at any point during the recovery.[18] Although FA, a measure used to characterize the integrity of tissue microstructure by computing the degree of difference among eigenvalues, is a commonly used variable in neuroradiology, the utility of FA in musculoskeletal tissue in an injured state may be less clear. This may be due to a smaller relative difference of the axial versus radial diffusivities in muscle compared to the brain, and thus decreased sensitivity of FA in muscle. Further, the discrepancy between the significant relationship detected between eccentric strength and λ_1, but not λ_2 and λ_3, indicates that the physiological difference between λ_1 (diffusion along the longitudinal axis) and λ_2 and λ_3 (diffusion in the transverse directions), may be a driving factor between the relationships identified with each eigen value and eccentric strength.

Interestingly, despite the positive relationship between muscle volume and strength being widely accepted,[68] we did not observe an association of between-limb differences in total hamstring or primary injured muscle volume and the between-limb difference in eccentric strength. Prior studies have demonstrated that DTI was able to identify muscle microstructure differences related to back muscle strength that were not reflected by gross muscle morphology, such as cross-sectional area.[74] Additionally, we did not detect a relationship between edema volume and eccentric strength between-limb difference at RTS. Thus, DTI may potentially identify subtle changes in hamstring muscle microstructure that relate to muscle strength that are not captured by gross muscle morphology.

Finally, previous work has demonstrated DTI tractography analyses of hamstring musculature are sensitive to changes in a targeted strengthening program for a healthy population, with a significant change in length detected in the semitendinosus muscle and in fascicle orientation in the BFlh.[77] To our knowledge, tractography of the hamstring muscles in an injured population has not yet been reported; however, ultrasound derived measures of fascicle length demonstrate decreased BFlh fascicle length in those with a previous HSI, while the relationship between fascicle orientation and injury is less clear.[97] In the present study, although the majority of injuries were of the BFlh, a significant relationship between fascicle length and eccentric strength limb differences was not detected. This may be due to the semitendinosus being more heavily recruited than the BFlh during the Nordic hamstring exercise.[98, 99] Thus, the method used to measure eccentric strength in this study may be less sensitive to changes of the BFlh specifically and additional exploration of DTI to detect relationships between fascicle length and eccentric strength following HSI, across all hamstring muscles, may be warranted.

Reinjury

Of the 20 index HSIs, 4 (20%) went on to reinjure within 12-months. Consistent with a recent review,[50] our findings failed to demonstrate that RTS MRI-based measurements at the gross-anatomical level are associated with reinjury. Similarly, a significant relationship between DTI parameters at the intermediate tissue-organ level and reinjury status was not detected in the present analysis. Although imaging conducted at RTS provides insight into muscle morphology near the completion of the recovery process, it does not account for the tissue loads and adaptations that may continue with prolonged exposure to prior activity levels beyond RTS. While imaging measures at RTS may still hold relevant relationships with long-term outcomes following HSI, future studies will need a rigorous study design to account for external factors and challenges associated with the RTS time point, such as timing relative to the competitive season and relative tissue loads and exposure at/beyond RTS. Consideration of interval assessments during recovery, independent of RTS, and through early exposure to prolonged levels of prior activity levels may be warranted.

Limitations

To the best of our knowledge, this is the first investigation to include comprehensive assessment of quantitative imaging measures and clinical outcomes such as eccentric hamstring strength and reinjury incidence following acute HSI. Despite the utility of this dataset, the relationship of the diffusion tensor in the presence of injury is complex due to the limited specificity of DTI measures in the presence of edema.[25] However, DTI measures in the presence of injury do still demonstrate validity.[18, 25] Further, imaging the muscle in a recovered state at RTS, with a significant decrease in the extracellular fluid consistent with edema, minimizes this complexity. Limitations exist in the identification of the injured region based on voxels containing increased signal intensity on T2-weighted imaging at the TOI and registering the estimated injured regions to follow up time points. However, a consensus on best

methods to identified the primary injured region do not exist and subtle between-limb differences in quantitative parameters would likely be undetectable if averaged across the entire muscle or muscle group. Additionally, HSIs are known to be multifactorial,[50] and although the focus of this study was to characterize the relationships between advanced, quantitative imaging and clinical outcomes, the investigation of potential interactions between imaging measures and additional risk factors such as prior injury and exposure after RTS is warranted. Finally, although the sample size of injuries and reinjury rate observed in the present study is consistent with prior prospective studies,[10, 13] accounting for an extensive list of potential contributing factors to explain clinical outcomes, especially reinjury following HSI, will require a larger sample with adequate power.

Conclusions

In conclusion, a significant association was detected between increased diffusivity measures (λ_1, MD) and eccentric strength deficits at the time of RTS following an acute HSI. The detection of a significant relationship between strength and diffusivity measures, but not gross-anatomical measures of muscle morphology, indicates that DTI may potentially track subtle changes in hamstring muscle microstructure that relate to muscle strength that are not captured by conventional imaging. Additional work is warranted to further understand the relationship between quantitative MRI parameters and reinjury status at standard intervals throughout recovery and beyond RTS.

Chapter 5.

Summary

The purpose of this thesis was to implement diffusion tensor imaging (DTI) to monitor muscle microstructure changes following acute hamstring strain injury (HSI) and throughout recovery. We explored the association of quantitative muscle morphology measures and DTI-derived measures of microstructure with clinical outcomes such as time to return to sport (RTS), eccentric hamstring strength, and reinjury incidence. While early applications of DTI demonstrate that it may identify subtle changes in microstructure undetected by conventional imaging in the context of muscle damage,[1, 2] procedures for the implementation of these methods following muscle injury are not well defined. Muscle strain injuries, specifically of the hamstrings, are prevalent yet complicated by limited prognostic indicators and high rates of reinjury. The implementation of a sensitive, quantitative measure to characterize muscle tissue after HSI may provide additional insight toward improving the clinical management of HSIs.

This work demonstrated that defining the injured region based on increased signal within the hamstring muscle on T2-weighted images obtained at the time of injury (TOI), and registering this region to images collected at follow-up time points, holds promise in describing muscle microstructure following HSI. When using this approach to define the injured region, between limb differences in DTI-derived measures of hamstring muscle microstructure were detected at TOI but not at RTS or 12-weeks after RTS. Identification of between limb differences immediately following injury that resolve at RTS and beyond is consistent with changes expected with healing. The resolution of between limb differences in DTI-derived measures despite the continued presence of edema at follow-up time points suggests that DTI may provide distinct information from information derived from T2-weighted imaging alone.

None of the quantitative MRI-based measures obtained at TOI (British Athletic Muscle Injury Classification, muscle edema volume, or DTI-derived measures) were associated with

time to RTS. Similarly, the measures derived from conventional T1- and T2-weighted imaging did not demonstrate a significant association with reinjury. However, those who went on to reinjure demonstrated decreased quantitative diffusion parameters within the injured muscle at TOI compared to those who do not reinjure. The direction of this relationship was unexpected, as increased diffusion is consistent with a more severe injury and thus it was hypothesized that these subjects would be at more at risk for reinjury. These findings may be a result of external factors not captured by TOI imaging, such as the state of muscle microstructure at RTS or the relative loads the tissue was exposed to at or beyond RTS. Analysis of microstructure at RTS provided further insight into this relationship and demonstrated that the between limb comparison of DTI-derived parameters (mean diffusivity, radial diffusivity, and principal effective diffusivity eigenvalue λ_1) held a significant association with between-limb eccentric hamstring strength values. Conversely, between-limb measures of muscle morphology were not associated with eccentric strength.

Collectively, these findings indicate that DTI-derived measures of muscle microstructure averaged over the injured region defined by increased signal on a T2-weighted image can be used to describe expected between limb differences immediately following and throughout recovery from acute HSI. Further, significant correlations between inferred measures of muscle microstructure identified with DTI and eccentric strength at the time of RTS indicate that DTI may be a valid measure to explore the known relationship to exist between muscle structure and function. The resolution of between limb microstructural differences despite the presence of continued edema at RTS, and the identified relationship between clinical measures of muscle function and microstructure, but not morphology, indicate that DTI may be more sensitive to structural changes following injury than measures derived from conventional imaging. The association of DTI measures with reinjury status following HSI remains unclear. Future work to

improve the validity, robustness, and efficiency of these methods to further explore the clinical translation of DTI for the management of HSI is warranted.

Future work

While the methods used in this thesis demonstrated DTI can be used describe expected changes in muscle microstructure and plausible associations of the structure and function relationship following HSI, additional work is warranted to address the validity and improve the robustness and efficiency of DTI in injured muscle prior to considering the clinical translation of these methods. The next logical steps toward the advancement of DTI for monitoring muscle microstructure following injury include advancements in the technical aspects of the acquisition and post-processing required for diffusion weighted imaging of injured muscle and improvements in the study design used to further explore the clinical associations of these measures.

While the spin-echo echo planer imaging sequence used for the acquisition of diffusion weighted imaging in this thesis proved adequate to reveal subtle changes in DTI parameters of skeletal muscle and was feasible to collect data from a large muscle group such as the hamstrings, implementation of advanced techniques to improve the specificity of DTI to measure microstructural changes in the presence of injury. Acquisition protocols with more averaging or increased diffusion-gradient directions[28, 32] to increase signal-to-noise ratio or angular resolution, as well as multi-shell diffusion imaging[23-25] or utilizing muscle specific model fitting[44] may be advantageous to better understand the complex relationship of the diffusion tensor fit in the presence of injury. Combining diffusion with quantitative relaxometry techniques such as multi-exponential T2 quantitative mapping[25] may offer additional insight into interpretation of microstructural changes that cannot be inferred from diffusion alone. Although multi-shell diffusion imaging may hold the most promise in resolving microstructural changes derived from the tensor fit data of DTI, this application has not been well studied in

muscle *in vivo* due to its two greatest drawbacks, scan duration and the non-trivial technique required to fit multi-shell T2 data.[25] Further investigation and implementation of multi-shell diffusion imaging is warranted to improve the interpretation of DTI-derived parameters following muscle strain injuries.

Another challenge faced by the acquisition protocols used in this work was the need for multiple slabs necessary to acquire data along the length of a large muscle group such as the hamstrings. Although the primary outcome measures discussed throughout this thesis were related to the scalar DTI measures, muscle fascicle length derived from tractography was also explored but was limited by the blending of DWI data across multiple slabs. Implementation of more robust measures of data acquisition will also positively impact the post-processing required for tractography, however, additional post-processing techniques such as slice artifact corrections via constrained neural networks[100] could be implemented to specifically improve blending across slabs. The utilization of AIR™ Recon DL developed by GE HealthCare (Chicago, IL) also holds early promise in improving the signal-to-noise ratio of reconstructed diffusion weighted imaging data[101] which may improve blending of diffusion data across slabs for tractography methods. GE HealthCare has provided us with funding support to explore this novel reconstruction method for the improvement of diffusion weighted imaging for muscle. Data collection and preliminary analysis for this follow-up study is already underway.

While technical advancements in image acquisition and processing for diffusion weighted imaging is warranted, improvements in the study design implemented for the work included in this thesis would be valuable to further understand the clinical associations explored in this thesis. An increased sample size with adequate power to detect a true difference in measures of muscle microstructure between athletes who do versus do not go on to reinjure would be beneficial to further explore the unexpected findings of decreased quantitative diffusion parameters consistent with a less severe injury at TOI compared to those who do not reinjure. Imaging data utilized within this thesis was a part of a larger study adequately powered

for the primary aims of the study not related to diffusion weighted imaging as preliminary evidence for diffusion-based measures of muscle microstructure following HSI did not exist at the time. Mean and standard deviation values from the datasets used in this thesis can be used to conduct an appropriate sample size analysis with adequate power to detect differences in DTI-derived measures of muscle microstructure between those who do versus do not go on to reinjure following HSI. Using the between limb percent difference values of the principal effective diffusivity eigenvalue λ_1 at TOI (reinjury: 5.23 $\pm$2.07%, no reinjury: 10.6 $\pm$7.46%) and RTS (reinjury: 5.11 $\pm$4.01%, no reinjury: 3.13 $\pm$3.82%), sample size analyses for two sample t-test powered at 0.8 resulted in required sample sizes of 66 and 244 athletes at TOI and RTS, respectively, to detect statistically meaningful differences between those that do versus do not go on to reinjure. While these numbers are large, the prevalence of HSI makes these sample sizes attainable, especially if implemented in a multi-center study across multiple institutions or organizations.

An additional study design consideration for future work would be the implementation of subsequent imaging sessions at routine intervals, in addition to imaging data collected at TOI and RTS. Due to the known multifactorial nature of HSI,[50] it is likely that external factors unrelated to the clinical state of the muscle structure or function may influence the decision for RTS and thus effect the time to RTS. While larger sample sizes may be able to account for the interaction of external factors, such as the starter status of the athlete or the timing of the injury relative to the competitive season, interval imaging on a weekly basis may also provide additional insight into the healing process of muscle microstructure independent of clinical decisions and external factors influencing RTS.

Finally, better understanding of normative DTI parameters of the hamstrings in a healthy population may help to define regional differences within and across hamstring muscles. This would be beneficial to interpret the clinical versus statistical significance of the relationships identified in this thesis work, and may provide further guidance for methods to explore muscle

microstructure for athletes who present with clinical findings of HSI but no evidence of injury on conventional T1- and T2-weighted imaging.

Ultimately, the work included in this thesis indicates DTI may be a sensitive measure to detect changes in muscle microstructure following HSI that are more closely linked with clinical outcomes, such as eccentric strength, than measures of muscle morphology observed with conventional imaging. As research related to the implementation of DTI for muscle continues to expand and more robust and efficient techniques for the acquisition and post-processing of this data are identified, future studies with a more rigorous study design may hold potential to work towards the clinical translation of DTI to improve the management of HSIs.

References

1. Froeling, M., et al., *Muscle changes detected with diffusion-tensor imaging after long-distance running.* Radiology, 2015. **274**(2): p. 548-62.
2. Hooijmans, M.T., et al., *Quantitative MRI Reveals Microstructural Changes in the Upper Leg Muscles After Running a Marathon.* J Magn Reson Imaging, 2020. **52**(2): p. 407-417.
3. Guermazi, A., et al., *Imaging of Muscle Injuries in Sports Medicine: Sports Imaging Series.* Radiology, 2017. **285**(3): p. 1063.
4. de Mello, R., et al., *Quantitative MRI Musculoskeletal Techniques: An Update.* AJR Am J Roentgenol, 2019. **213**(3): p. 524-533.
5. Mueller-Wohlfahrt, H.W., et al., *Terminology and classification of muscle injuries in sport: the Munich consensus statement.* Br J Sports Med, 2013. **47**(6): p. 342-50.
6. Pollock, N., et al., *British athletics muscle injury classification: a new grading system.* Br J Sports Med, 2014. **48**(18): p. 1347-51.
7. Valle, X., et al., *Muscle Injuries in Sports: A New Evidence-Informed and Expert Consensus-Based Classification with Clinical Application.* Sports Med, 2017. **47**(7): p. 1241-1253.
8. Chan, O., et al., *Acute muscle strain injuries: a proposed new classification system.* Knee Surg Sports Traumatol Arthrosc, 2012. **20**(11): p. 2356-62.
9. Cohen, S.B., et al., *Hamstring injuries in professional football players: magnetic resonance imaging correlation with return to play.* Sports Health, 2011. **3**(5): p. 423-30.
10. Biglands, J.D., et al., *MRI in acute muscle tears in athletes: can quantitative T2 and DTI predict return to play better than visual assessment?* Eur Radiol, 2020. **30**(12): p. 6603-6613.
11. Tears, C., et al., *The British Athletics Muscle Injury Classification grading system as a predictor of return to play following hamstrings injury in professional football players.* Phys Ther Sport, 2022. **58**: p. 46-51.
12. Pollock, N., et al., *Time to return to full training is delayed and recurrence rate is higher in intratendinous ('c') acute hamstring injury in elite track and field athletes: clinical application of the British Athletics Muscle Injury Classification.* Br J Sports Med, 2016. **50**(5): p. 305-10.
13. McAuley, S., et al., *Predictors of time to return to play and re-injury following hamstring injury with and without intramuscular tendon involvement in adult professional footballers: A retrospective cohort study.* J Sci Med Sport, 2022. **25**(3): p. 216-221.
14. Shamji, R., et al., *Association of the British Athletic Muscle Injury Classification and anatomic location with return to full training and reinjury following hamstring injury in elite football.* BMJ Open Sport Exerc Med, 2021. **7**(2): p. e001010.
15. Wangensteen, A., et al., *MRI does not add value over and above patient history and clinical examination in predicting time to return to sport after acute hamstring injuries: a prospective cohort of 180 male athletes.* Br J Sports Med, 2015. **49**(24): p. 1579-87.
16. Wangensteen, A., et al., *New MRI muscle classification systems and associations with return to sport after acute hamstring injuries: a prospective study.* Eur Radiol, 2018. **28**(8): p. 3532-3541.
17. Oudeman, J., et al., *Techniques and applications of skeletal muscle diffusion tensor imaging: A review.* J Magn Reson Imaging, 2016. **43**(4): p. 773-88.
18. Monte, J.R., et al., *Diffusion tensor imaging and quantitative T2 mapping to monitor muscle recovery following hamstring injury.* NMR Biomed, 2023: p. e4902.
19. Zaraiskaya, T., D. Kumbhare, and M.D. Noseworthy, *Diffusion tensor imaging in evaluation of human skeletal muscle injury.* J Magn Reson Imaging, 2006. **24**(2): p. 402-8.

20. Giraudo, C., et al., *Normalized STEAM-based diffusion tensor imaging provides a robust assessment of muscle tears in football players: preliminary results of a new approach to evaluate muscle injuries.* Eur Radiol, 2018. **28**(7): p. 2882-2889.
21. Karampinos, D.C., et al., *Considerations in high-resolution skeletal muscle diffusion tensor imaging using single-shot echo planar imaging with stimulated-echo preparation and sensitivity encoding.* NMR Biomed, 2012. **25**(5): p. 766-78.
22. Damon, B.M., et al., *Skeletal muscle diffusion tensor-MRI fiber tracking: rationale, data acquisition and analysis methods, applications and future directions.* NMR Biomed, 2017. **30**(3).
23. Ababneh, Z., et al., *Biexponential parameterization of diffusion and T2 relaxation decay curves in a rat muscle edema model: decay curve components and water compartments.* Magn Reson Med, 2005. **54**(3): p. 524-31.
24. Fan, R.H. and M.D. Does, *Compartmental relaxation and diffusion tensor imaging measurements in vivo in lambda-carrageenan-induced edema in rat skeletal muscle.* NMR Biomed, 2008. **21**(6): p. 566-73.
25. Berry, D.B., et al., *Relationships between tissue microstructure and the diffusion tensor in simulated skeletal muscle.* Magn Reson Med, 2018. **80**(1): p. 317-329.
26. Martin-Noguerol, T., et al., *A handbook for beginners in skeletal muscle diffusion tensor imaging: physical basis and technical adjustments.* Eur Radiol, 2022. **32**(11): p. 7623-7631.
27. Mattiello J, B.P., Lebihan D., *Analytical expressions for the b-matrix in NMR diffusion imaing an spectroscopy.* J Magn Reson, 1994. **108**: p. 131-141.
28. Froeling, M., et al., *DTI of human skeletal muscle: the effects of diffusion encoding parameters, signal-to-noise ratio and T2 on tensor indices and fiber tracts.* NMR Biomed, 2013. **26**(11): p. 1339-52.
29. Kuo, G.P. and J.A. Carrino, *Skeletal muscle imaging and inflammatory myopathies.* Curr Opin Rheumatol, 2007. **19**(6): p. 530-5.
30. Bolsterlee, B., A. D'Souza, and R.D. Herbert, *Reliability and robustness of muscle architecture measurements obtained using diffusion tensor imaging with anatomically constrained tractography.* J Biomech, 2019. **86**: p. 71-78.
31. Pierpaoli, C. and P.J. Basser, *Toward a quantitative assessment of diffusion anisotropy.* Magn Reson Med, 1996. **36**(6): p. 893-906.
32. Damon, B.M., *Effects of image noise in muscle diffusion tensor (DT)-MRI assessed using numerical simulations.* Magn Reson Med, 2008. **60**(4): p. 934-44.
33. Andersson, J.L., S. Skare, and J. Ashburner, *How to correct susceptibility distortions in spin-echo echo-planar images: application to diffusion tensor imaging.* Neuroimage, 2003. **20**(2): p. 870-88.
34. Andersson, J.L.R. and S.N. Sotiropoulos, *An integrated approach to correction for off-resonance effects and subject movement in diffusion MR imaging.* Neuroimage, 2016. **125**: p. 1063-1078.
35. Manjon, J.V., et al., *Diffusion weighted image denoising using overcomplete local PCA.* PLoS One, 2013. **8**(9): p. e73021.
36. Forsting, J., et al., *Diffusion tensor imaging of the human thigh: consideration of DTI-based fiber tracking stop criteria.* MAGMA, 2020. **33**(3): p. 343-355.
37. Esposito, A., et al., *Magnetic resonance imaging at 7T reveals common events in age-related sarcopenia and in the homeostatic response to muscle sterile injury.* PLoS One, 2013. **8**(3): p. e59308.
38. Silldorff, M.D., et al., *Effect of supraspinatus tendon injury on supraspinatus and infraspinatus muscle passive tension and associated biochemistry.* J Bone Joint Surg Am, 2014. **96**(20): p. e175.

39. Hamer, P.W., et al., *Evans Blue Dye as an in vivo marker of myofibre damage: optimising parameters for detecting initial myofibre membrane permeability.* J Anat, 2002. **200**(Pt 1): p. 69-79.
40. Taylor, D.C., et al., *Experimental muscle strain injury. Early functional and structural deficits and the increased risk for reinjury.* Am J Sports Med, 1993. **21**(2): p. 190-4.
41. Timmins, R.G., et al., *Architectural adaptations of muscle to training and injury: a narrative review outlining the contributions by fascicle length, pennation angle and muscle thickness.* Br J Sports Med, 2016. **50**(23): p. 1467-1472.
42. Keller, S., et al., *Diffusion tensor imaging combined with T2 mapping to quantify changes in the skeletal muscle associated with training and endurance exercise in competitive triathletes.* Eur Radiol, 2020. **30**(5): p. 2830-2842.
43. Sciorati, C., et al., *7-Tesla magnetic resonance imaging precisely and noninvasively reflects inflammation and remodeling of the skeletal muscle in a mouse model of antisynthetase syndrome.* Biomed Res Int, 2014. **2014**: p. 879703.
44. Sigmund, E.E., et al., *Time-dependent diffusion in skeletal muscle with the random permeable barrier model (RPBM): application to normal controls and chronic exertional compartment syndrome patients.* NMR Biomed, 2014. **27**(5): p. 519-28.
45. Ekstrand, J., M. Hagglund, and M. Walden, *Epidemiology of muscle injuries in professional football (soccer).* Am J Sports Med, 2011. **39**(6): p. 1226-32.
46. Darrow, C.J., et al., *Epidemiology of severe injuries among United States high school athletes: 2005-2007.* Am J Sports Med, 2009. **37**(9): p. 1798-805.
47. Ekstrand, J., et al., *Risk factors for hamstring muscle injury in male elite football: medical expert experience and conclusions from 15 European Champions League clubs.* BMJ Open Sport Exerc Med, 2023. **9**(1): p. e001461.
48. Liu H, G.W., Moorman CT, Yu B. , *Injury rate, mechanism, and risk factors of hamstring strain injuries in sports: A review of the literature.* Journal of Sport and Health Science, 2012. **1**(2): p. 92-101.
49. Hickey, J., et al., *The financial cost of hamstring strain injuries in the Australian Football League.* Br J Sports Med, 2014. **48**(8): p. 729-30.
50. Green, B., et al., *Recalibrating the risk of hamstring strain injury (HSI): A 2020 systematic review and meta-analysis of risk factors for index and recurrent hamstring strain injury in sport.* Br J Sports Med, 2020. **54**(18): p. 1081-1088.
51. Opar, D.A., M.D. Williams, and A.J. Shield, *Hamstring strain injuries: factors that lead to injury and re-injury.* Sports Med, 2012. **42**(3): p. 209-26.
52. de Visser, H.M., et al., *Risk factors of recurrent hamstring injuries: a systematic review.* Br J Sports Med, 2012. **46**(2): p. 124-30.
53. Hallen, A. and J. Ekstrand, *Return to play following muscle injuries in professional footballers.* J Sports Sci, 2014. **32**(13): p. 1229-36.
54. Kerkhoffs, G.M., et al., *Diagnosis and prognosis of acute hamstring injuries in athletes.* Knee Surg Sports Traumatol Arthrosc, 2013. **21**(2): p. 500-9.
55. Reurink, G., et al., *Magnetic resonance imaging in acute hamstring injury: can we provide a return to play prognosis?* Sports Med, 2015. **45**(1): p. 133-46.
56. Reurink, G., et al., *MRI observations at return to play of clinically recovered hamstring injuries.* Br J Sports Med, 2014. **48**(18): p. 1370-6.
57. Greenky, M. and S.B. Cohen, *Magnetic resonance imaging for assessing hamstring injuries: clinical benefits and pitfalls - a review of the current literature.* Open Access J Sports Med, 2017. **8**: p. 167-170.
58. Rudisill, S.S., et al., *Evidence-Based Management and Factors Associated With Return to Play After Acute Hamstring Injury in Athletes: A Systematic Review.* Orthop J Sports Med, 2021. **9**(11): p. 23259671211053833.

59. Jacobsen, P., et al., *A combination of initial and follow-up physiotherapist examination predicts physician-determined time to return to play after hamstring injury, with no added value of MRI.* Br J Sports Med, 2016. **50**(7): p. 431-9.
60. McAleer, S., et al., *Time to return to full training and recurrence of rectus femoris injuries in elite track and field athletes 2010-2019; a 9-year study using the British Athletics Muscle Injury Classification.* Scand J Med Sci Sports, 2022. **32**(7): p. 1109-1118.
61. van Heumen, M., et al., *The prognostic value of MRI in determining reinjury risk following acute hamstring injury: a systematic review.* Br J Sports Med, 2017. **51**(18): p. 1355-1363.
62. Heiderscheit, B.C., et al., *Hamstring strain injuries: recommendations for diagnosis, rehabilitation, and injury prevention.* J Orthop Sports Phys Ther, 2010. **40**(2): p. 67-81.
63. Maniar, N., et al., *Hamstring strength and flexibility after hamstring strain injury: a systematic review and meta-analysis.* Br J Sports Med, 2016. **50**(15): p. 909-20.
64. Ribeiro-Alvares, J.B., et al., *Eccentric knee flexor strength of professional football players with and without hamstring injury in the prior season.* Eur J Sport Sci, 2021. **21**(1): p. 131-139.
65. Sanfilippo, J.L., et al., *Hamstring strength and morphology progression after return to sport from injury.* Med Sci Sports Exerc, 2013. **45**(3): p. 448-54.
66. Kocak, U.Z., M.R. Stiffler-Joachim, and B.C. Heiderscheit, *Comparison of eccentric hamstring strength and asymmetry at return-to-sport after hamstring strain injury among those who did and did not re-injure.* Phys Ther Sport, 2023. **59**: p. 25-29.
67. Silder, A., et al., *MR observations of long-term musculotendon remodeling following a hamstring strain injury.* Skeletal Radiol, 2008. **37**(12): p. 1101-9.
68. Lieber, R.L. and J. Friden, *Functional and clinical significance of skeletal muscle architecture.* Muscle Nerve, 2000. **23**(11): p. 1647-66.
69. Lieber, R.L. and J. Friden, *Clinical significance of skeletal muscle architecture.* Clin Orthop Relat Res, 2001(383): p. 140-51.
70. Silder, A., et al., *Clinical and morphological changes following 2 rehabilitation programs for acute hamstring strain injuries: a randomized clinical trial.* J Orthop Sports Phys Ther, 2013. **43**(5): p. 284-99.
71. De Vos, R.J., et al., *Clinical findings just after return to play predict hamstring re-injury, but baseline MRI findings do not.* Br J Sports Med, 2014. **48**(18): p. 1377-84.
72. Isern-Kebschull, J., et al., *MRI findings prior to return to play as predictors of reinjury in professional athletes: a novel decision-making tool.* Insights Imaging, 2022. **13**(1): p. 203.
73. Vermeulen, R., et al., *Complete resolution of a hamstring intramuscular tendon injury on MRI is not necessary for a clinically successful return to play.* Br J Sports Med, 2020.
74. Klupp, E., et al., *Paraspinal Muscle DTI Metrics Predict Muscle Strength.* J Magn Reson Imaging, 2019. **50**(3): p. 816-823.
75. Scheel, M., et al., *Diffusion tensor imaging of skeletal muscle--correlation of fractional anisotropy to muscle power.* Rofo, 2013. **185**(9): p. 857-61.
76. Takao, S., et al., *Diffusion tensor imaging (DTI) of human lower leg muscles: correlation between DTI parameters and muscle power with different ankle positions.* Jpn J Radiol, 2022. **40**(9): p. 939-948.
77. Suskens, J.J.M., et al., *Effect of two eccentric hamstring exercises on muscle architectural characteristics assessed with diffusion tensor MRI.* Scand J Med Sci Sports, 2023. **33**(4): p. 393-406.
78. Van Donkelaar, C.C., et al., *Diffusion tensor imaging in biomechanical studies of skeletal muscle function.* J Anat, 1999. **194 (Pt 1)**(Pt 1): p. 79-88.

79. Napadow, V.J., et al., *Quantitative analysis of three-dimensional-resolved fiber architecture in heterogeneous skeletal muscle tissue using nmr and optical imaging methods.* Biophys J, 2001. **80**(6): p. 2968-75.
80. Jenkinson, M., et al., *Fsl.* Neuroimage, 2012. **62**(2): p. 782-90.
81. McCarthy, P., *FSLeyes*. 2022, Zenodo.
82. Jenkinson, M., et al., *Improved optimization for the robust and accurate linear registration and motion correction of brain images.* Neuroimage, 2002. **17**(2): p. 825-41.
83. Hooijmans, M.T., et al., *Evaluation of skeletal muscle DTI in patients with duchenne muscular dystrophy.* NMR Biomed, 2015. **28**(11): p. 1589-97.
84. Okamoto, Y., et al., *Diffusion property differences of the lower leg musculature between athletes and non-athletes using 1.5T MRI.* MAGMA, 2012. **25**(4): p. 277-84.
85. Koo, T.K. and M.Y. Li, *A Guideline of Selecting and Reporting Intraclass Correlation Coefficients for Reliability Research.* J Chiropr Med, 2016. **15**(2): p. 155-63.
86. Shrout, P.E. and J.L. Fleiss, *Intraclass correlations: uses in assessing rater reliability.* Psychol Bull, 1979. **86**(2): p. 420-8.
87. Weir, J.P., *Quantifying test-retest reliability using the intraclass correlation coefficient and the SEM.* J Strength Cond Res, 2005. **19**(1): p. 231-40.
88. Handsfield, G.G., et al., *Relationships of 35 lower limb muscles to height and body mass quantified using MRI.* J Biomech, 2014. **47**(3): p. 631-8.
89. Crema, M.D., et al., *Hamstring Injuries in Professional Soccer Players: Extent of MRI-Detected Edema and the Time to Return to Play.* Sports Health, 2018. **10**(1): p. 75-79.
90. Kumaravel, M., P. Bawa, and N. Murai, *Magnetic resonance imaging of muscle injury in elite American football players: Predictors for return to play and performance.* Eur J Radiol, 2018. **108**: p. 155-164.
91. Gibbs, N.J., et al., *The accuracy of MRI in predicting recovery and recurrence of acute grade one hamstring muscle strains within the same season in Australian Rules football players.* J Sci Med Sport, 2004. **7**(2): p. 248-58.
92. Fang, Q. *Iso2Mesh*. 2021 [cited 2021 September 29]; Available from: https://github.com/fangq/iso2mesh.
93. Yeh, F.C., et al., *Deterministic diffusion fiber tracking improved by quantitative anisotropy.* PLoS One, 2013. **8**(11): p. e80713.
94. Ward, S.R., et al., *Are current measurements of lower extremity muscle architecture accurate?* Clin Orthop Relat Res, 2009. **467**(4): p. 1074-82.
95. Opar, D.A., et al., *A novel device using the Nordic hamstring exercise to assess eccentric knee flexor strength: a reliability and retrospective injury study.* J Orthop Sports Phys Ther, 2013. **43**(9): p. 636-40.
96. Deux, J.F., et al., *Assessment of calf muscle contraction by diffusion tensor imaging.* Eur Radiol, 2008. **18**(10): p. 2303-10.
97. Kellis, E. and C. Sahinis, *Is Muscle Architecture Different in Athletes with a Previous Hamstring Strain? A Systematic Review and Meta-Analysis.* J Funct Morphol Kinesiol, 2022. **7**(1).
98. Hegyi, A., et al., *Region-dependent hamstrings activity in Nordic hamstring exercise and stiff-leg deadlift defined with high-density electromyography.* Scand J Med Sci Sports, 2018. **28**(3): p. 992-1000.
99. Bourne, M.N., et al., *Impact of exercise selection on hamstring muscle activation.* Br J Sports Med, 2017. **51**(13): p. 1021-1028.
100. Pietsch, M., et al., *dStripe: Slice artefact correction in diffusion MRI via constrained neural network.* Med Image Anal, 2021. **74**: p. 102255.
101. Peters, R.L., S., *AIR Recon DL for diffusion weighted imaging.* . 2021: gehealthcare.com.